LBNL-41914

Ernest Orlando Lawrence Berkeley National Laboratory

Nonlinear Interaction of Plane Elastic Waves

Valeri A. Korneev, Kurt T. Nihei, and Larry R. Myer

Earth Sciences Division

June 1998

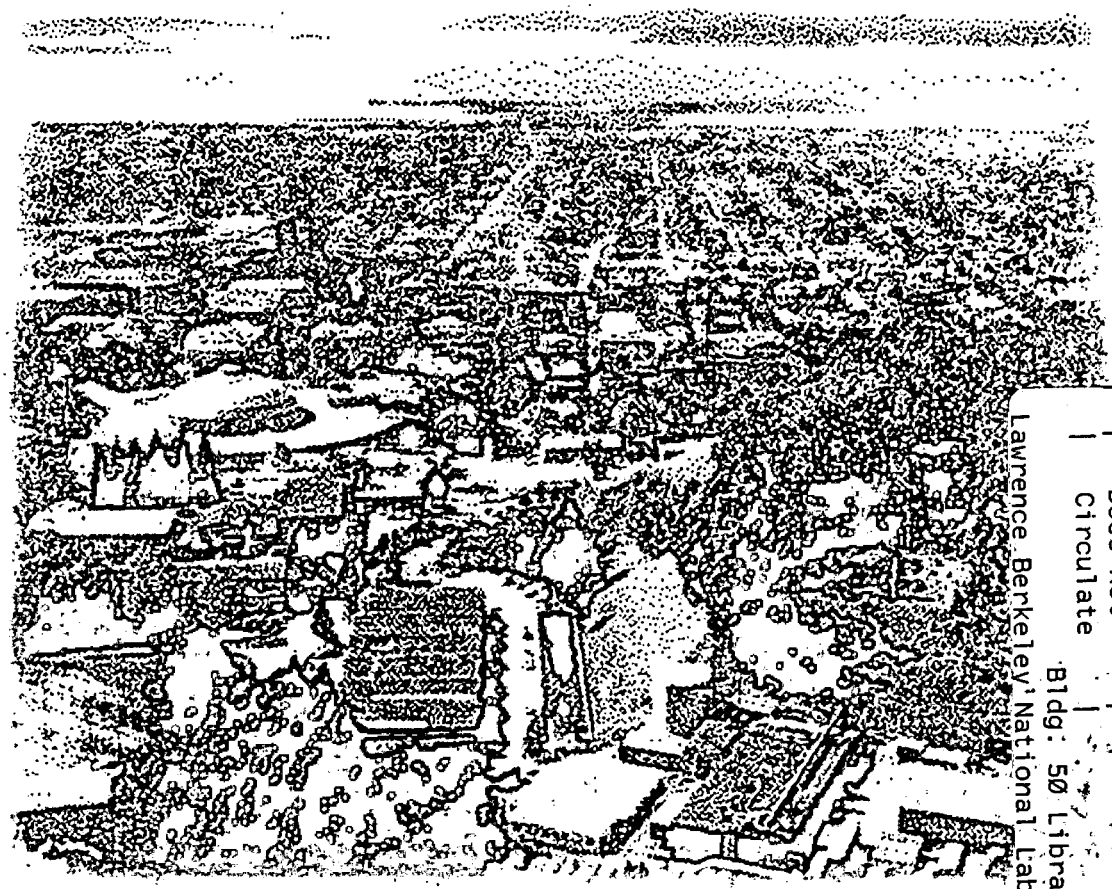

REFERENCE COPY
Does Not
Circulate
Bldg. 50 Library - Ref.
Lawrence Berkeley National Laboratory
Copy 1
LBNL-41914

DISCLAIMER

This document was prepared as an account of work sponsored by the United States Government. While this document is believed to contain correct information, neither the United States Government nor any agency thereof, nor the Regents of the University of California, nor any of their employees, makes any warranty, express or implied, or assumes any legal responsibility for the accuracy, completeness, or usefulness of any information, apparatus, product, or process disclosed, or represents that its use would not infringe privately owned rights. Reference herein to any specific commercial product, process, or service by its trade name, trademark, manufacturer, or otherwise, does not necessarily constitute or imply its endorsement, recommendation, or favoring by the United States Government or any agency thereof, or the Regents of the University of California. The views and opinions of authors expressed herein do not necessarily state or reflect those of the United States Government or any agency thereof or the Regents of the University of California.

LBNL-41914

Nonlinear Interaction of Plane Elastic Waves

Valeri A Korneev, Kurt T Nihei and Larry R Myer

Earth Sciences Division
Ernest Orlando Lawrence Berkeley National Laboratory
University of California
Berkeley , California 94720

June 1998

This study was supported by the Director, Office of the Energy Research, Office of Basic Energy Sciences, Engineering and Geosciences Division of the U.S. Department of Energy under Contract No. DE-AC03-76SF00098.

1. Summary

Paper presents basic first order results of nonlinear elastic theory by Murnaghan for elastic wave propagation in isotropic solids. We especially address to the problem of resonant scattering of two collimated beams and present analytical solutions for amplitudes of all possible types of resonant interactions for elastic plane waves. For estimation of nonlinear scattered waves we use measured elastic parameters for sandstone. The most profound nonlinear effect is expected for interactions of two SH waves generating compressional P wave at sum frequency. Our estimations show that nonlinear phenomena is likely to be observed in seismic data. Basic equations of nonlinear five-constant theory by Murnaghan are also presented.

Key words: nonlinear, interaction, elastic, wave propagation.

2. Introduction

Nonlinearity is any deviation from the linear law of the transformation of the input signal due to its propagation through a carrying system. Nonlinearity may appear in the signal at all stages starting from elastic waves excitation , then during propagation of waves through elastic material, in registration device and also in the stage of numerical data processing. We consider in this paper nonlinearity arising due to properties of elastic material.

As is well known the complete form of the strain tensor contains squared terms and assumptions about the smallness of strains are needed to get a linear equation of elastic motion. Nonlinear systems of differential equations result if other physical phenomena associated with elastic deformation, such as heat conduction, electromagnetic field generation, dislocations, material flow, viscosity, and strain-stress

hysteresis, are also taken into account. Microcracks in rock may close due to transient stress imposed by propagating elastic waves. In this case the boundary conditions for the wave propagation problem become dependent upon the amplitude of the wave. Elastic nonlinearity of different materials, including rock samples has been observed for ultrasonic frequencies by many authors (Breazeale and Thompson, 1963; Carr , 1964,1966 ; Ermilin at al., 1970; Gedroits and Krasil'nikov, 1963; Moriamez et. al., 1968; Thery et. al. , 1969, Johnson et. al.,1993). In particular it has been shown that velocity of elastic waves changes with static deformation and hydrostatic pressure. Waves of mixed frequencies as a result of nonlinear wave interaction have also been reported (Rollins et. al.,1964; Zarembo and Krasil'nikov, 1971; Johnson et. al.,1987; Johnson and Shankland, 1989). The fundamental equations of nonlinear elastic theory by Murnaghan effectively describe such classical nonlinear phenomena as harmonics generation and resonant wave scattering. Results of this theory are well known among solid state physicists, but most of the information is scattered. Probably the most comprehensive description of the theory can be found in the monograph of Zarembo and Krasil'nikov (1966), published in Russian. Evidence of nonlinearity is reported in many experimental publications for solid materials and crystals. Some estimates for rocks (Meegan et al, 1993) show large levels of nonlinearity, which has lead to a growing interest to this phenomena among seismologists. Besides basic equations this paper presents correct solutions for all possible types of nonlinear interactions of collimated beams in the volume of nonlinear elastic material. These solutions in combination with background theory of plane wave propagation in nonlinear media may help to design an experimental research in nonlinear seismology.

3. Basic equations of the five-constant theory of elastic nonlinearity

The general problem of finite deformations in elastic solids was developed by Novozhilov (1948) and Murnaghan (1951), who derived stress-strain relations considering conditions of equilibrium and the virtual work of any virtual deformation inside the elastic medium. These results were used for experimental laboratory measurements of nonlinear elastic constants for a set of isotropic and crystalline materials by Hughes and Kelly, 1953. Later Landau and Lifshitz (1954) suggested the way of derivation of nonlinear equations of motion using the internal elastic energy function and its relation with the

stress tensor. This derivation was made by Goldberg (1961) and described most completely in the book of Zarembo and Krasil'nikov (1966). It has been used by most authors and is the basis for the following.

Assuming elastic deformation in a solid, and that the displacement vector,

$$\mathbf{u} = \mathbf{u}(x,y,z) = \mathbf{u}(x_1,x_2,x_3) = \left[u_1(x_1,x_2,x_3)\ ,\ u_2(x_1,x_2,x_3)\ ,\ u_3(x_1,x_2,x_3)\right]$$

is continuous together with its spatial partial derivatives, the corresponding strain tensor is defined as:

$$u_{ik} = \frac{1}{2}\left[\frac{\partial u_i}{\partial x_k} + \frac{\partial u_k}{\partial x_i} + \frac{\partial u_l}{\partial x_k}\frac{\partial u_l}{\partial x_i}\right] \tag{1}$$

which has three invariants:

$$I_1 = u_{ii}$$

$$I_2 = \frac{1}{2}(u_{ss}^2 - u_{ik}^2) \tag{2}$$

$$I_3 = \left|u_{ik}\right| = \frac{1}{3}\left[u_{ik}u_{is}u_{ks} - \frac{3}{2}u_{ik}^2 u_{ss} + \frac{1}{2}u_{ss}^3\right]$$

(Here and later repeated index means summation.)

If it is assumed that the strain components are small, it is possible to show (Landau and Lifshitz, 1953) that in the coordinate system of undeformed solid the stress tensor is defined by:

$$\sigma_{ik} = \frac{\partial U}{\partial\left[\dfrac{\partial u_i}{\partial x_k}\right]} \tag{3}$$

where U is the internal elastic energy for adiabatic deformations. The internal energy of the isotropic solid is invariant under coordinate transformation. Since it is a function only of the deformation of the body (dissipative processes are neglected and deformations are assumed to be ideally elastic), the internal energy must depend only on the invariants of the strain tensor:

$$U = U(I_1\ ,I_2\ ,I_3) \tag{4}$$

Representing this function by the first terms of a Taylor expansion we get

$$U = U(0,0,0) + \frac{\partial U}{\partial I_1} I_1 + \left[\frac{\partial U}{\partial I_2} I_2 + \frac{1}{2} \frac{\partial^2 U}{\partial I_1^2} I_1^2 \right]$$

$$+ \left[\frac{\partial U}{\partial I_3} I_3 + \frac{1}{2} \frac{\partial^2 U}{\partial I_1 \partial I_2} I_1 I_2 + \frac{1}{6} \frac{\partial^3 U}{\partial I_1^3} I_1^3 \right] \tag{5}$$

with the accuracy of cubic degree in the strain tensor components. All partial derivations in (5) are assumed to be calculated in the undeformed state, where $U(0,0,0) = 0$. Equilibrium in the undeformed state also gives

$$\frac{\partial U}{\partial I_1} = 0$$

The other partial derivations in (5) can be expressed as:

$$\frac{\partial U}{\partial I_2} = -2\mu \ , \qquad \frac{\partial U}{\partial I_3} = n = A \ , \qquad \frac{\partial^2 U}{\partial I_1^2} = \lambda + 2\mu$$

$$\frac{\partial^2 U}{\partial I_1 \partial I_2} = -4m = -2A - 4B \tag{6}$$

$$\frac{\partial^3 U}{\partial I_1^3} = 4m + 2l = 2A + 6B + 2C$$

where λ , μ are Lame constants, l, m, n are nonlinear elastic constants of the third order introduced by Murnaghan and A, B, C are the constants introduced by Landau and Lifshitz. The constants l, m, n, A, B, C will heretofore be called simply *nonlinear constants*

The constants l, m, n and A, B, C are related in the following way:

$$l = B + C \ , \qquad A = n \ , \tag{7}$$

$$m = \frac{A}{2} + B \ , \qquad B = m - \frac{n}{2}$$

$$n = A \ , \qquad C = l - m + \frac{n}{2}$$

Following previous papers of Gol'dberg (1961),Kobett and Jones (1963) we will use the constants A, B, C. The internal elastic energy can therefore be written as:

$$U = \mu u_{ik} + \frac{\lambda}{2} u_{ss}^2 + \frac{A}{3} u_{ik} u_{is} u_{ks} + B u_{ik}^2 u_{ss} + \frac{C}{3} u_{ss}^3 \tag{8}$$

Substituting components of the strain tensor (1) into (8) it is possible to obtain:

$$U = \frac{\mu}{4}\left[\frac{\partial u_i}{\partial x_k} + \frac{\partial u_k}{\partial x_i}\right]^2 + \frac{\lambda}{2}\left[\frac{\partial u_s}{\partial x_s}\right]^2 + \left[\mu + \frac{A}{4}\right]\frac{\partial u_i}{\partial x_k}\frac{\partial u_s}{\partial x_i}\frac{\partial u_s}{\partial x_k} + \frac{(B+\lambda)}{2}\frac{\partial u_s}{\partial x_s}\left[\frac{\partial u_i}{\partial x_k}\right]^2$$

$$+ \frac{A}{12}\frac{\partial u_i}{\partial x_k}\frac{\partial u_k}{\partial x_s}\frac{\partial u_s}{\partial x_i} + \frac{B}{2}\frac{\partial u_i}{\partial x_k}\frac{\partial u_k}{\partial x_i}\frac{\partial u_s}{\partial x_s} + \frac{C}{3}\left[\frac{\partial u_s}{\partial x_s}\right]^3 \tag{9}$$

where all components of degree higher than 3 have been neglected.

The equation of motion in an perfectly elastic solid is given by:

$$\rho\frac{\partial^2 u_i}{\partial t^2} = \frac{\partial \sigma_{ik}}{\partial x_k} \tag{10}$$

where σ_{ik} are components of the stress tensor (3).

Using (9) and (3) it is possible to obtain the relation between stress and strain components:

$$\sigma_{ik} = \mu\left[\frac{\partial u_i}{\partial x_k} + \frac{\partial u_k}{\partial x_i}\right] + \lambda\frac{\partial u_s}{\partial x_s}\delta_{ik} + \left[\mu + \frac{A}{4}\right]\left[\frac{\partial u_s}{\partial x_i}\frac{\partial u_s}{\partial x_k} + \frac{\partial u_k}{\partial x_s}\frac{\partial u_i}{\partial x_s} + \frac{\partial u_s}{\partial x_k}\frac{\partial u_i}{\partial x_s}\right] +$$

$$\frac{(B+\lambda)}{2}\left[\left[\frac{\partial u_s}{\partial x_j}\right]^2\delta_{ik} + 2\frac{\partial u_i}{\partial x_k}\frac{\partial u_s}{\partial x_s}\right] + \frac{A}{4}\frac{\partial u_k}{\partial x_s}\frac{\partial u_s}{\partial x_i} +$$

$$\frac{B}{2}\left[\frac{\partial u_s}{\partial x_j}\frac{\partial u_j}{\partial x_s}\delta_{ik} + 2\frac{\partial u_k}{\partial x_i}\frac{\partial u_s}{\partial x_s}\right] + C\left[\frac{\partial u_s}{\partial x_s}\right]^2\delta_{ik} \tag{11}$$

which is a generalized Hook's law.

Considering the presence of dissipative forces by introducing coefficients η and ζ for shear and volume viscosities, respectively (Landau and Lifshitz, 1953), and substituting (11) in (10) we have the equation of motion in the form:

$$\rho\frac{\partial^2 U_i}{\partial t^2} - \mu\frac{\partial^2 u_i}{\partial x_k^2} - (\lambda+\mu)\frac{\partial^2 u_k}{\partial x_k \partial x_i} - \frac{\partial}{\partial t}\left[\eta\frac{\partial^2 u_i}{\partial x_k^2} - \left[\zeta + \frac{\eta}{3}\right]\frac{\partial^2 u_k}{\partial x_k \partial x_i}\right] = F_i \tag{12}$$

where F_i, the i^{ith} component of **F**, has a value of the second order in smallness and is given by:

$$F_i = C_1\left[\frac{\partial^2 u_s}{\partial x_k^2}\frac{\partial u_s}{\partial x_i} + \frac{\partial^2 u_s}{\partial x_k^2}\frac{\partial u_i}{\partial x_s} + 2\frac{\partial^2 u_i}{\partial x_s \partial x_k}\frac{\partial u_s}{\partial x_k}\right] + C_2\left[\frac{\partial^2 u_s}{\partial x_i \partial x_k}\frac{\partial u_s}{\partial x_k} + \frac{\partial^2 u_k}{\partial x_s \partial x_k}\frac{\partial u_i}{\partial x_s}\right]$$

$$+ C_3 \frac{\partial^2 u_i}{\partial x_k^2} \frac{\partial u_s}{\partial x_s} + C_4 \left[\frac{\partial^2 u_k}{\partial x_s \partial x_k} \frac{\partial u_s}{\partial x_i} + \frac{\partial^2 u_s}{\partial x_i \partial x_k} \frac{\partial u_k}{\partial x_s} \right] + C_5 \frac{\partial^2 u_k}{\partial x_i \partial x_k} \frac{\partial u_s}{\partial x_s}$$

$$+ \frac{\partial}{\partial t} \left[\eta \frac{\partial u_s}{\partial x_i} \frac{\partial^2 u_s}{\partial x_k^2} - \left(\zeta + \frac{\eta}{3} \right) \frac{\partial u_s}{\partial x_k} \frac{\partial^2 u_s}{\partial x_k \partial x_i} \right] \tag{13}$$

where the following notation is used:

$$C_1 = \mu + \frac{A}{4}, \qquad C_2 = \lambda + \mu + \frac{A}{4} + B, \qquad C_3 = \frac{A}{4} + B$$

$$C_4 = B + 2C, \qquad C_5 = \lambda + B \tag{14}$$

The equation of motion (12) together with expression (13) is the basic result of so-called five-constant nonlinear elastic theory by Murnaghan. From (13) it is seen that components F_i do not become zero when the nonlinear constants are zero. This is a result of nonlinearity of the strain tensor (1), and means that, in general, nonlinear elastic solutions approach linear elastic solutions only when the strain components go to zero. On the other hand, for most solids, values of the nonlinear constants (A,B,C) are significantly larger than those of Lame constants λ,μ which usually may be neglected in coefficients (14).

If the next terms of the fourth order in expression (5) for elastic energy are considered it is necessary to introduce another four nonlinear constants, and so on. Some theoretical (Zabolotskaya, 1986) and experimental (Meegan et al, 1993) papers indicate that the fourth order terms in (5) could be important. However in this study the five-constant theory is used, assuming also that the strain components are small enough to provide F_i much smaller than any of components from left hand side of (12).

The relative smallness of F_i allows one to assume displacements can be written in the following form:

$$\mathbf{u} = \mathbf{u}_0 + \mathbf{u}_1 + \ldots \tag{15}$$

where $\mathbf{u}_0$ is a solution of homogeneous equation (12) when F_i equals zero. Putting (15) into (12) and assuming that $|\mathbf{u}_0| \gg |\mathbf{u}_1|$ we can get a linear equation for $\mathbf{u}_1$ where the left hand side contains com-

ponents of $\mathbf{u}_1$ and the right hand side, F_i, depends on the previously determined function $\mathbf{u}_0$, only. In the next section this method will be applied to the problem of propagation of harmonic elastic plane waves in an isotropic homogeneous nonlinear medium.

4. Nonlinear propagation of the plane elastic waves

The basic ideas of the phenomena of elastic wave propagation in nonlinear medium may be found in Landau and Lifshitz, (1953), where the phenomena of generation of waves of multiple frequencies are described. Details of nonlinear propagation of originally single elastic waves can be found in papers of (Gol'dberg, 1960; Polyakova, 1964; Zarembo and Krasil'nikov, 1966,1970, McCall, 1993), from which the next general results were obtained.

P-plane wave propagation. In this case the equation for determination of $\mathbf{u}_1$ is an inhomogeneous resonance equation and we must include attenuation to obtain a finite solution. The solution to the homogeneous equation for an incident plane p-wave propagation along the x-axis is:

$$\mathbf{u}_0 = u_0 \exp^{-a_p x} \cos(k_p x - \omega t)\, \hat{\mathbf{x}} \tag{16}$$

where

$$a_p = \frac{\left[\frac{4}{3}\eta + \zeta\right]\omega^2}{2\rho v_p^3}$$

is the attenuation coefficient. Medium nonlinearity causes generation of the second compressional harmonic $\mathbf{u}_1$ which has the form

$$\mathbf{u}_1 = \frac{u_0^2 \beta_0 \omega^2}{8 a_p v_p^2}\left[\exp^{-2a_p x} - \exp^{-4a_p x}\right] \cos 2(k_p x - \omega t)\, \hat{\mathbf{x}} \tag{17}$$

where the following notation is used

$$k_p = \frac{\omega}{v_p}\ , \quad v_p = \sqrt{\frac{\lambda + 2\mu}{\rho}}\ , \quad \beta_0 = \frac{3(\lambda + 2\mu) + 2(2m + l)}{2(\lambda + 2\mu)} \tag{18}$$

At a distance $x = ln\, 2/2a$ the second harmonic (17) reaches a maximum and then decreases.

S-plane wave propagation. This wave excites secondary p-waves, but does not generate any s-waves. Taking $\mathbf{u}_0$ as the plane s-wave:

$$\mathbf{u}_0 = u_0 \exp^{-a_s x} \cos(k_s x - \omega t)\, \hat{\mathbf{y}} \tag{19}$$

the secondary p-wave polarized in x- direction has the form:

$$\mathbf{u}_1 = \frac{u_0^2 \gamma_0 \omega v_p^2}{4 v_s (v_s^2 - v_p^2)} \left[\exp^{-4a_p x} \sin 2(k_p x - \omega t) - \exp^{-2a_s x} \sin 2(k_s x - \omega t) \right] \hat{\mathbf{x}} \tag{20}$$

where

$$a_s = \frac{\eta \omega^2}{2 \rho v_s^3}$$

is the attenuation coefficient of the shear waves and

$$k_s = \frac{\omega}{v_s}, \qquad v_s = \sqrt{\frac{\mu}{\rho}}, \qquad \gamma_0 = \frac{\lambda + 2\mu + m}{2(\lambda + 2\mu)}$$

When $a_p x$, $a_s x$ $\ll 1$ expression (20) reduces to:

$$\mathbf{u}_1 = \frac{u_0^2 \gamma_0 \omega v_p^2}{2 v_s (v_s^2 - v_p^2)} \sin x (k_s - k_p) \cdot \cos\left[(k_p + k_s) x - 2\omega t \right] \hat{\mathbf{x}} \tag{21}$$

The wave represented by (21) evidentially has spatial modulation with period

$$\Delta x = \frac{\pi v_p v_s}{\omega (v_p - v_s)} \tag{22}$$

This period has the order of the wavelength in the medium. The second harmonic given by eq. (21) is small because the length of wave interaction is small (of order one wavelength), and nonlinear effects do not accumulate. The resonant accumulation of the second harmonic for S wave may still occur if one considers fourth order terms in (5) due to interaction of the third harmonic with primary wave (Zabolotskaya, 1986).

Propagation of the secondary waves causes generation of harmonics of higher orders. Amplitudes of these multiple harmonics decrease rapidly with increasing harmonic number. As discussed in the next section, however, the chance to observe the nonlinearity of the elastic medium appears to improve for

the case of nonlinear interaction of elastic waves of different primary frequencies.

5. Nonlinear interaction of elastic waves

Under some circumstances elastic waves of different frequencies ω_1 and ω_2 propagating in a solid may interact and produce secondary waves of mixed (sum or difference) frequencies ω_r. Theoretically this problem is similar to phonon-phonon interactions, a subject of quantum mechanics. The conditions when such resonant interactions may exist are:

$$\omega_r = \omega_1 \pm \omega_2 \tag{23'}$$

$$\mathbf{k}_r = \mathbf{k}_1 \pm \mathbf{k}_2 \tag{23''}$$

where (23") includes the corresponding wave vectors. The + sign in (23) corresponds to the case of sum resonant frequencies and the - sign corresponds to the case of difference resonant frequencies. Therefore condition (23') defines the frequencies of scattered waves, and condition (23") defines their direction of propagation. In the case of a liquid medium without dispersion, condition (23") means that interaction is possible for collinear waves only. For solids, due to the existence of two velocities of propagation, a variety of different resonance interactions become possible. The geometry of sum resonance interaction is illustrated in Fig.1, and for difference interaction is in Fig.2. The angle α of interactions is given by:

$$\left[\frac{\omega_r}{v_r}\right]^2 = \left[\frac{\omega_1}{v_1}\right]^2 + \left[\frac{\omega_2}{v_2}\right]^2 \pm 2\frac{\omega_1}{v_1}\frac{\omega_2}{v_2}\cos\alpha \tag{24}$$

which is the result of (23"). Velocities v_r, v_1, v_2 might be equal to either v_p or v_s depending on the type of interaction. Equation (24) together with conditions

$$-1 \le \cos\alpha \le 1 \tag{25}$$

cannot be satisfied for all possible combinations of waves and frequencies, which means that some types of interactions do not exist.

Angle ψ of propagation of the resonant wave defined by geometry in Fig. 1,2 can be found from:

$$tg\,\psi = \frac{\pm\frac{v_1}{v_2}d\cdot\sin\alpha}{1 \pm \frac{v_1}{v_2}d\cos\alpha} \tag{26}$$

where

$$d = \frac{\omega_2}{\omega_1} \tag{27}$$

Basic results of the interaction of elastic waves in an isotropic solid were obtained by Jones and Kobett (1963), Taylor and Rollings (1964), Zarembo and Krasil'nikov (1971). The displacement field of the sum of two incident plane waves:

$$\mathbf{u}_0 = \mathbf{u}_0^{(1)} + \mathbf{u}_0^{(2)} = \mathbf{A}_0 cos(\omega_1 t - \mathbf{k}_1\mathbf{r}) + \mathbf{B}_0 cos(\omega_2 t - \mathbf{k}_2\mathbf{r}) \tag{28}$$

with amplitudes A_0 and B_0 respectively, are substituted into the equation of motion (12) assuming no presence of attenuation. Denoting by **p** that part of **F** from (13) which describes the interaction of waves, (28) can be written in the form

$$\mathbf{p}(\mathbf{r},t) = \mathbf{\Gamma}^+ \sin[(\omega_1 + \omega_2)t - (\mathbf{k}_1 + \mathbf{k}_2)\mathbf{r}] + \mathbf{\Gamma}^- \sin[(\omega_1 - \omega_2)t - (\mathbf{k}_1 - \mathbf{k}_2)\mathbf{r}] \tag{29}$$

where

$$\begin{aligned}
\mathbf{\Gamma}^{\pm} = & -\frac{1}{2}C_1[(\mathbf{A}_0\mathbf{B}_0)(\mathbf{k}_2\mathbf{k}_2)\mathbf{k}_1 \pm (\mathbf{A}_0\mathbf{B}_0)(\mathbf{k}_1\mathbf{k}_1)\mathbf{k}_2 + (\mathbf{B}_0\mathbf{k}_1)(\mathbf{k}_2\mathbf{k}_2)\mathbf{A}_0 \pm (\mathbf{A}_0\mathbf{k}_2)(\mathbf{k}_1\mathbf{k}_1)\mathbf{B}_0 + \\
& 2(\mathbf{A}_0\mathbf{k}_2)(\mathbf{k}_1\mathbf{k}_2)\mathbf{B}_0 \pm 2(\mathbf{B}_0\mathbf{k}_1)(\mathbf{k}_1\mathbf{k}_2)\mathbf{A}_0] \\
& -\frac{1}{2}C_2[(\mathbf{A}_0\mathbf{B}_0)(\mathbf{k}_1\mathbf{k}_2)\mathbf{k}_2 \pm (\mathbf{A}_0\mathbf{B}_0)(\mathbf{k}_1\mathbf{k}_2)\mathbf{k}_1 + (\mathbf{B}_0\mathbf{k}_2)(\mathbf{k}_1\mathbf{k}_2)\mathbf{A}_0 \pm (\mathbf{A}_0\mathbf{k}_1)(\mathbf{k}_1\mathbf{k}_2)\mathbf{B}_0] \\
& -\frac{1}{2}C_3[(\mathbf{A}_0\mathbf{k}_2)(\mathbf{B}_0\mathbf{k}_2)\mathbf{k}_1 \pm (\mathbf{A}_0\mathbf{k}_1)(\mathbf{B}_0\mathbf{k}_1)\mathbf{k}_2 + (\mathbf{A}_0\mathbf{k}_2)(\mathbf{B}_0\mathbf{k}_1)\mathbf{k}_2 \pm (\mathbf{A}_0\mathbf{k}_2)(\mathbf{B}_0\mathbf{k}_1)\mathbf{k}_1] \\
& -\frac{1}{2}C_4[(\mathbf{A}_0\mathbf{k}_1)(\mathbf{B}_0\mathbf{k}_2)\mathbf{k}_2 \pm (\mathbf{A}_0\mathbf{k}_1)(\mathbf{B}_0\mathbf{k}_2)\mathbf{k}_1] - \frac{1}{2}C_5[(\mathbf{A}_0\mathbf{k}_1)(\mathbf{k}_2\mathbf{k}_2)\mathbf{B}_0 \pm (\mathbf{B}_0\mathbf{k}_2)(\mathbf{k}_1\mathbf{k}_1)\mathbf{A}_0]
\end{aligned} \tag{30}$$

Expressions of the form (xy) in (30) denote scalar products.

If there is a volume V inside the medium where the primary beams are well collimated, and if it is assumed that waves interact only in this volume it is possible to obtain a solution for the scattered secondary field in the far field:

$$\mathbf{u}_1(\mathbf{r},t) = \frac{(\mathbf{\Gamma}^+\hat{\mathbf{r}})\hat{\mathbf{r}}}{4\pi v_p^2 \rho r} \int_V \sin\left[\left(\frac{\omega_1 + \omega_2}{v_p}\hat{\mathbf{r}} - \mathbf{k}_1 - \mathbf{k}_2\right)\cdot\mathbf{r}' - (\omega_1 + \omega_2)\left(\frac{r}{v_p} - t\right)\right] dV \quad +$$

$$\frac{(\mathbf{I}^-\hat{\mathbf{r}})\hat{\mathbf{r}}}{4\pi v_p^2 \rho r}\int_V \sin\left[\left(\frac{\omega_1-\omega_2}{v_p}\hat{\mathbf{r}}-\mathbf{k}_1+\mathbf{k}_2\right)\cdot\mathbf{r}' - (\omega_1-\omega_2)\left(\frac{r}{v_p}-t\right)\right]dV \quad +$$

$$\frac{\mathbf{I}^+-(\mathbf{I}^+\hat{\mathbf{r}})\hat{\mathbf{r}}}{4\pi v_s^2 \rho r}\int_V \sin\left[\left(\frac{\omega_1+\omega_2}{v_s}\hat{\mathbf{r}}-\mathbf{k}_1-\mathbf{k}_2\right)\cdot\mathbf{r}' - (\omega_1+\omega_2)\left(\frac{r}{v_s}-t\right)\right]dV \quad +$$

$$\frac{\mathbf{I}^--(\mathbf{I}^-\hat{\mathbf{r}})\hat{\mathbf{r}}}{4\pi v_s^2 \rho r}\int_V \sin\left[\left(\frac{\omega_1-\omega_2}{v_s}\hat{\mathbf{r}}-\mathbf{k}_1+\mathbf{k}_2\right)\cdot\mathbf{r}' - (\omega_1-\omega_2)\left(\frac{r}{v_s}-t\right)\right]dV \qquad (31)$$

where $\mathbf{r} = r\hat{\mathbf{r}}$; $|\hat{\mathbf{r}}| = 1$ is the radius-vector from the center point of the interaction region and observation point; $\mathbf{r}'$ is the radius-vector of integration inside the volume V (geometry shown on Fig.3) .

The first and second terms in (31) are compressional waves with the sum frequency $\omega_1 + \omega_2$ and the difference frequency $\omega_1-\omega_2$, respectively. The third and fourth terms are shear waves with the sum and difference frequencies, respectively. As we integrate over $\mathbf{r}'$ all the integrands in (31) oscillate with frequencies determined by the coefficients of $\mathbf{r}'$ and the results of any integration will depend on just how the waves fit into the region V. Scattered waves have natural polarizations: parallel to $\mathbf{r}$ for p-waves and orthogonal to $\mathbf{r}$ for s-waves. Integrals in (31) are referred to as volume factors.

If we satisfy resonant conditions (23) by chosing an appropriate direction $\hat{\mathbf{r}} = \hat{\mathbf{r}}_r$ the corresponding coefficient of $\mathbf{r}'$ becomes equal to zero and the amplitude of the scattered wave in this direction becomes proportional to the volume, V, of integration.

From (31) it also follows that amplitudes of the scattered waves are proportional to their projections in the direction $\mathbf{n}$, where $\mathbf{n}$ is the unit vector of the natural polarization of the wave. For P-waves $\mathbf{n}$ is parallel to $\hat{\mathbf{r}}$ and for S-waves it is perpendicular. This means that the resonant scattering amplitude may be zero even if resonant conditions (23) are satisfied. A zero scattering amplitude due to polarization will be referred to as polarization restriction.

All of the types of elastic wave resonant interactions are shown in Table 1, where sign " $\times$ " means that interaction is possible and sign " $\rightarrow$ " means that interaction is possible only when interacting waves are collinear. All other types of interactions are forbidden. Sign " O " marks interactions which are forbidden because of polarization restrictions; all others are forbidden because resonant

conditions (23) for them can not be satisfied. Only 10 of 54 interactions are possible. Sum frequency resonance exists only for compressional scattered waves for the following interactions:

$$
\begin{aligned}
P(\omega_1) + P(\omega_2) &= P(\omega_1 + \omega_2) \\
P(\omega_1) + SV(\omega_2) &= P(\omega_1 + \omega_2) \\
SV(\omega_1) + P(\omega_2) &= P(\omega_1 + \omega_2) \\
SV(\omega_1) + SV(\omega_2) &= P(\omega_1 + \omega_2) \\
SH(\omega_1) + SH(\omega_2) &= P(\omega_1 + \omega_2)
\end{aligned}
\tag{32}
$$

Interactions 2 and 3 in (32) are reciprocal. We regard them here as two different interactions keeping the structure of Tab.1.

Difference frequency resonance is possible for the following interactions:

$$
\begin{aligned}
P(\omega_1) + P(\omega_2) &= P(\omega_1 - \omega_2) \\
P(\omega_1) + P(\omega_2) &= SV(\omega_1 - \omega_2) \\
P(\omega_1) + SV(\omega_2) &= P(\omega_1 - \omega_2) \\
P(\omega_1) + SV(\omega_2) &= SV(\omega_1 - \omega_2) \\
P(\omega_1) + SH(\omega_2) &= SH(\omega_1 - \omega_2)
\end{aligned}
\tag{33}
$$

A similar table for forbidden and allowed scattering processes for an isotropic solid published in the paper of Zarembo and Krasil'nikov (1971) contained 18 possible interactions. We believe their results are partly in error. Taylor and Rollins (1964) present five possible interactions omitting the problem of separation of *SV* and *SH* polarization for shear waves.

If resonant conditions (23) are satisfied for any one type of interaction the scattered field from (31) may be rewritten in the form

$$
\mathbf{u}_1(\mathbf{r},t) = G_g^{\pm} \sin\left[(\omega_1 \pm \omega_2)(t - \frac{r}{v_g})\right]\cdot\mathbf{n} \tag{34}
$$

where $g = p$ or $g = s$ depending from the type of the scattering wave and $\mathbf{n}$ is the unit vector of the

natural polarization for this wave. Function $G_g^{\pm}$ is the resonant scattering amplitude, which may be calculated using the expressions

$$G_g^{\pm} = \frac{(\mathbf{I}^{\pm}\mathbf{n})}{4\pi v_g^2 \rho} \frac{V}{r} = W_g^{\pm} \left[\frac{\omega_1}{v_p}\right]^3 \frac{V}{r} A_0 B_0 , \quad A_0 = |\mathbf{A}_0| , \quad B_0 = |\mathbf{B}_0| \tag{35}$$

with nondimensional nonlinear amplitude coefficient

$$W_g^{\pm} = \frac{(\mathbf{I}^{\pm}\mathbf{n})}{4\pi v_g^2 \rho A_0 B_0} \left[\frac{v_p}{\omega_1}\right]^3 \tag{36}$$

Analytical expressions for W_g of all ten possible scattering interactions are shown in Table 2 together with expressions for interacting angle, α, and limits, $d_{\min}$, $d_{\max}$, of the frequency ratio $d = \frac{\omega_2}{\omega_1}$. In addition the following notation is used:

$$D = \frac{d}{4\pi(\lambda + 2\mu)} , \qquad \gamma = \sqrt{\frac{\mu}{\lambda+2\mu}} = \frac{v_s}{v_p} \tag{37}$$

Approximate expressions for scattering amplitudes in Table 2 are derived from exact formulas using the assumption that we may neglect Lame constants λ , μ in terms in C_i (eq. 13) containing nonlinear constants A, B, C. The results in Table 2 reveal rather simple dependence of scattering amplitudes on the nonlinear elastic constants. Amplitudes of two collinear PP interactions are proportional to $2m + l$; six interactions are proportional to m and not dependent on other constants. The remaining two interactions, where SH waves are involved, have more complicated dependence on constants m and n .

Calculations were done for a set of nonlinear elastic parameters representative of a typical rock (sandstone) as follows:

$$\lambda = 4.14\ GPa , \qquad m = -3.66 \cdot 10^3 GPa$$

$$\mu = 7.36\ GPa , \qquad l = -1.11 \cdot 10^4 GPa$$

$$\rho = 2.3\ g/cm^3 , \qquad n = 8.71 \cdot 10^4 GPa$$

These nonlinear parameters were derived from laboratory P- and S-wave velocity measurements on core as described in Appendix I.

Plots of the functions $W_g^{\pm}(d)$, where $d = \frac{\omega_2}{\omega_1}$ are presented in Fig. 4.1 - 4.7 together with interaction angle α and absolute value of the scattered angle ψ. We don't show here results for collinear P- waves propagation as having trivial dependence on frequency, as well as for mentioned above interaction $SV(\omega_1) + P(\omega_2) = P(\omega_1 + \omega_2)$ since it is reciprocal with interaction $P(\omega_1) + SV(\omega_2) = P(\omega_1 + \omega_2)$. Results based on the formulas in Table 2 revealed coincidence with those obtained by direct computations using vector form (30).

As seen in the figures there are several values of d for which $W_g = 0$. These roots do not depend on nonlinear constants. For the interaction $P(\omega_1) + P(\omega_2) = SV(\omega_1 - \omega_2)$ there is one root given by:

$$d_0 = \frac{\omega_2}{\omega_1} = \frac{1}{1-\gamma^2}\left[1 - \gamma\sqrt{2-\gamma^2}\right]$$

The curve for interaction $P(\omega_1) + SV(\omega_2) = P(\omega_1 - \omega_2)$ has a root

$$d_0 = \frac{\omega_2}{\omega_1} = \frac{1}{1-\gamma^2}\left[\gamma\sqrt{2-\gamma^2} - \gamma^2\right]$$

Roots for other curves may be found as a solutions of relevant equations , which are polynomials of the fourth order. Two interactions containing SH waves theoretically may have roots for some combinations of nonlinear constants.

For most interactions there are bounds on the value of d for the existence of interactions. Only collinear interaction of P- waves for sum frequency gives infinite growth as frequency ratio d increases. All other interactions are limited for the whole range $d_{\min} \le d \le d_{\max}$ of its allowed variation. Except two collinear interactions and interaction $P(\omega_1) + P(\omega_2) = SV(\omega_1 - \omega_2)$ (Fig. 4.4) scattering may occur for the whole range of angles ψ . Two P-waves generate scattered P-waves with sum and difference frequencies only if the interacting waves are collinear.

The conditions under which the amplitude of the scattered waves are maxima are of practical interest in planning experiments to observe nonlinear phenomena. The figures show that these conditions are particular to each type of interaction. The amplitudes of the scattered waves at sum frequencies are, however, generally greater than those at difference frequencies. The greatest value of W_g for a difference frequency is about 95 for the interaction $P(\omega_1) + SH(\omega_2) \rightarrow SH(\omega_1 - \omega_2)$ while other maxima are less than 20. On the other hand, only one of the maxima for sum frequencies has a value as low as 95. All other maxima for sum frequencies are greater than 450 and, as noted above, two are unbounded. Though sum frequencies generally result in larger nonlinear amplitudes it should be noted that the effects of attenuation have not been considered in this analysis. Attenuations would preferentially tend to lessen the amplitudes of the sum frequencies. Attenuation would also result in bounds on the amplitudes of interactions such as $P(\omega_1) + P(\omega_2) \rightarrow P(\omega_1 - \omega_2)$.

6. Scattering beamwidth

The scattered waves given by (31) appear in the form of conical beams with vertexes at the interaction zone and maximum intensity in the direction $\mathbf{r}_r$, the unit vector in the direction of $\mathbf{k}_r$ (Eq. 23). To investigate the amplitudes of the scattering beams as a function of observation position let us assume that the interaction volume has the shape of a sphere of radius R . Any volume factor from (31) may then be reduced to the form:

$$V_f = \int_V \sin\left[a\cdot(\hat{\mathbf{r}}\cdot\mathbf{r}') - \Delta\right]dV = -\sin\Delta \int_0^{2\pi}\int_0^{R}\int_0^{\pi} \cos(a\cos\theta r)\sin\theta d\theta r^2 dr d\phi =$$

$$-\sin\Delta \frac{4\pi}{a_3}\int_0^{aR} \sin x\cdot x dx = -\sin\Delta\ V\cdot 3\frac{j_1(aR)}{aR} \tag{38}$$

where $V = \frac{4}{3}\pi R^3$, the volume of the sphere, $j_1(x)$ are spherical bessel functions of the first order, and Δ, which represents phase components of the volume factors, is given by:

$$\Delta = (\omega_1 \pm \omega_2)\left[\frac{r}{v_v} - t\right]$$

The coefficient a in eq. 38 is

$$a = \left| \frac{\omega_1 \pm \omega_2}{v_r} \hat{\mathbf{r}} - \mathbf{k}_1 \pm \mathbf{k}_2 \right| \tag{39}$$

If θ is the angle between resonant scattering direction $\mathbf{r}_r$ and observation direction $\hat{\mathbf{r}}$ we can write

$$\hat{\mathbf{r}} = \cos\theta\, \hat{\mathbf{r}} + \sin\theta\, \hat{\rho} \tag{40}$$

where $\hat{\rho}$ is a unit vector orthogonal to $\hat{\mathbf{r}}$. Substituting (40) in (39) and using resonant conditions (23) we finally have:

$$aR = \frac{\omega_1 \pm \omega_2}{v_r} R \sqrt{2(1-\cos\theta)} = 2\pi \frac{R}{\lambda_r} \sqrt{2(1-\cos\theta)} \tag{41}$$

where λ_r is a wavelength of the scattered wave. Assuming the interaction volume is spherical, this analysis shows that the volume factor, V_f is proportional to the volume of the sphere.

Using the asymptotic approximation:

$$j_1(x) \approx \frac{x}{3}\left[1 - \frac{x^2}{2\cdot 5} + \frac{x^4}{2\cdot 4\cdot 5\cdot 7} - \ldots\right]$$

for spherical bessel functions in (38) we may estimate the total beamwidth, θ_w, of the scattering beam where the amplitude of the scattering beam is not less than a half of its maximum. The result is

$$\theta_w \approx 2arccos\left[1 - \frac{1}{10}\left[\frac{\lambda_r}{R}\right]^2\right] \tag{42}$$

For small angles ($\theta_w < 0.1$) Eq. (42) reduces to

$$\theta_w \approx \frac{\lambda_r}{R} \tag{43}$$

Scattering diagrams for ratios $\frac{R}{\lambda_r} = 0.5, 2.0$ are shown in Fig. 5.1,5.2. Assuming a spherical interaction volume, Figures 5.1-5.2 show that the scattering pattern becomes sharper with growth of the ratio $\frac{R}{\lambda_r}$, where λ_r is the wavelength of the secondary scattered field. That is, for a given size of interaction volume, the width of the conical beam decreases as the wavelength of the scattered energy

increases. Numerical approach of interaction volume estimation for spherical waves was developed in (Beresnev, 1993).

7. Discussion

The results of elastic plane wave interactions provide a basis for studying the nonlinear behavior of real elastic materials. Nonlinear elastic effects are proportional to the nonlinear elastic constants and the appropriate frequency band does not depend at all on these constants. Thus there may be opportunities to create universal observation systems for study of nonlinearity of the real elastic media. An exception may arise in consideration of two possible interactions involving SH waves, for which nonlinear effects have more complicated dependence on the nonlinear constants. It is, of course, assumed that absolute values of the nonelastic constants are much more than those of the Lame constants, which is commonly observed in experimental studies on rock samples. Otherwise, nonlinear effects are very small and unlikely to be observed.

While there is no question that earth materials exhibit nonlinearity over a wide range of conditions, it is appropriate to ask whether it is likely that this nonlinearity in elastic properties is large enough to produce observable effects in geophysical activities such as exploration and engineering seismology. The intent of this discussion is not to provide an exhaustive analysis of this question, but rather a preliminary assessment of the potential for observable effects. To simplify our analysis we introduce strain levels of primary waves:

$$S_p = |div\, \mathbf{u}_0| \tag{44}$$

for P- waves , and

$$S_s = |rot\, \mathbf{u}_0| \tag{45}$$

for S- waves. In the preceding sections theory is presented for two cases: propagation of plane waves in a nonlinear material, and interaction of two plane waves in a nonlinear volume. The former case will be addressed first.

Single plane wave propagation nonlinearity has been reported in many papers (Breazeale and Thompson, 1963; Carr , 1964,1966 ; Ermilin at al., 1970; Gedroits and Krasil'nikov, 1963; Moriamez et. al., 1968; Thery et. al. , 1969, Johnson et. al.,1993) concerned ultrasonic laboratory studies. Our goal here is to get an estimation of nonlinear effect for seismic waves. From section 4 it is seen that elastic nonlinearity gives rise to secondary harmonic in one dimensional P- plane wave propagation. This harmonic would increase in amplitude indefinitely with distance were it not for attenuation.

The relative amplitude of the primary and secondary harmonics can be studied by calculating the ratio, referred to as the nonlinear ratio:

$$q_n = \frac{\overline{|\mathbf{u}_1|}}{\overline{|\mathbf{u}_0|}} = W_p S_p \tag{46}$$

where the bar signifies a time averaged value, $\mathbf{u}_1$ and $\mathbf{u}_0$ are given by (16) and (17), and nonlinear coefficient has a form

$$W_p = \frac{\beta_0 \omega}{8 a_p v_p}\left[\exp^{-a_p x} - \exp^{-3a_p x}\right] \tag{47}$$

When propagation distance x is not very large for dissipation processes to dominate , the nonlinear coefficient is

$$W_p = \frac{\beta_0 \omega x}{4 v_p} \tag{48}$$

and is proportional to x .

For S-waves, using eq. (17) and eq. (20) , the ratio becomes:

$$q_n = \frac{\overline{|\mathbf{u}_1|}}{\overline{|\mathbf{u}_0|}} = W_s S_s \tag{49}$$

where nonlinear coefficient

$$W_s = \frac{\gamma_0 \gamma^3}{4(1-\gamma^2)} e^{(a_s - 2a_p)x} \sqrt{1 + e^{-4a_p x} - 2e^{-2a_p x}\cos\left[2x(k_p - k_s)\right]} \tag{50}$$

has a spatial modulation. For small distances (50) can be reduced to the form

$$W_s = \frac{x \gamma_0 \gamma^3}{2(1-\gamma^2)} \sqrt{(k_p - k_s)^2 + (2a_p - a_s)^2} \tag{51}$$

Plots of W_p for P-waves and W_s for S-waves are given in Figures 6.1 and 6.2. Calculations were carried out for ω = 100 Hz and the values of nonlinear elastic constants for sandstone given in section 5. The various curves correspond to values of α_p and α_s ranging from 10^{-4} to 10^{-6}. Figure 6.1 shows that the value of W_p, and hence the amplitude of the secondary harmonics, for P-waves, increases for some distance and then decreases. The value of α_p determines the distance at which the amplitudes of the secondary harmonics begin to decrease. At smaller distances the amplitude of the harmonics is largely independent of the value of α_p.

The second harmonics generated by S-waves have only P-wave particle motion. Figure 6.2 shows that these harmonics exhibit spatial modulation. The amplitude of this modulation varies with attenuation, being smaller for large values of α_s ; it also decreases with distance as attenuation damps out the effect of the nonlinear properties. Contrary to behavior for the P-wave, the second harmonies of the S-wave reach maxima which are relatively insensitive to the value of attenuation. For any value of attenuation it is also seen that the magnitude of the S-wave harmonic amplitude ratio is smaller than that of the P-wave.

Using values of W_p from Figure 6.1 values of the relative amplitude of the secondary harmonics can be calculated for a 100 Hz wave propagating through sandstone with the nonlinear properties discussed previously. For example, at 1000 m the amplitude of the secondary harmonic would approach 1% of the primary assuming a strain level in the primary of 10^{-6} and an α_p of 5 x 10^{-6}. If α_p were only 5 x 10^{-5} or greater, the relative amplitude of the secondary harmonics would drop to less than 0.01% of the primary wave amplitude. If the strain level of the primary is 10^{-6}, the secondary harmonics produced by an S-wave would not exceed 0.005% of the primary for any value of α_s at any distance.

These calculations imply that the nonlinear elastic properties of sandstone will result in only minor perturbations in the seismic signature under many situations of practical interest in seismic exploration geophysics. However, it should be noted that there are earth materials (such as soils) which are likely to be much more nonlinear than sandstone and there are situations (earthquakes, explosions) in which larger strains may be expected, so that much larger effects than noted above may be possible.

Nonlinear interaction of intersecting elastic waves has been detected in solids (Rollins et. al.,1964; Zarembo and Krasil'nikov, 1971) and in the rock (Johnson et. al.,1987; Johnson and Shankland, 1989). Based on the discussion in section 5 the size of the nonlinear effects arising from interaction of waves in a nonlinear volume can be assessed using the same material parameters as for the plane wave case just discussed. Making an assumption that amplitudes of primary waves are equal so that $A_0 = B_0 = u_0$ we may use the functions $W_g^{\pm}$ to find the ratio of resonant scattering amplitude to primary wave amplitude. This ratio, $q_g^{\pm}$, called the "nonlinear amplitude ratio", is given as:

$$q_g^{\pm} = \frac{G_g^{\pm}}{u_0} = W_g^{\pm} u_0 \frac{V}{r}\left[\frac{\omega_1}{V_p}\right]^3 \tag{52}$$

Eq. (52) can be rewritten in the form:

$$q_p = W_p\left[\frac{\omega_1}{V_p}\right]^2 \frac{V}{r} S_p \tag{53}$$

for P-waves, and

$$q_s = W_s \gamma\left[\frac{\omega_1}{V_p}\right]^2 \frac{V}{r} S_s \tag{54}$$

for S-waves. As an example consider a case in which ω_1 is $2\pi(40)$ rad/sec., V_p = 3300 m/sec, V_s = 2000 m/sec, V = 1 x 10^7 m^3 and r = 200 m. Eqs (53) and (54) become:

$$q_p = (289) W\ S_p \tag{55}$$

$$q_s = (175)\ W\ S_s \tag{56}$$

For each of the scattering interactions shown in Figures 4.1 to 4.10 the magnitude of W varies as a function of d. For purposes of this discussion it is appropriate to pick maximum values of W. For example, for the interaction SH(ω_1) + SH(ω_2) $\rightarrow$ P(ω_1 + ω_2), it is seen from Figure 4.5 that $W_{max} \simeq 970$ for d $\simeq$ 3.1. Hence, equation (56) yields,

$$q_s = 2.8 \times 10^5\ S_s$$

For a strain rate of 10^{-6}, S_s = 0.28. Thus, though counter-intuitive, the theory predicts that two SH waves, one at 40 Hz and the other at 124 Hz, intersecting at an angle of about 135 ° will generate a P-

wave at 164 Hz with an amplitude 0.28 times as large as the primary wave at a strain level of 10^{-6}. If an experiment were performed at the frequencies of 40 and 124 Hz other permissible interactions include $SV(\omega_1) + SV(\omega_2) \rightarrow P(\omega_1 + \omega_2)$, $P(\omega_1) + SV(\omega_2) \rightarrow P(\omega_1 + \omega_2)$, $SV(\omega_1) + P(\omega_2) \rightarrow P(\omega_1 + \omega_2)$ and $P(\omega_1) + P(\omega_2) \rightarrow P(\omega_1 + \omega_2)$. Of these only the collinear P-wave scattering produces an effect of comparable magnitude.

There are questions about the practicality of achieving strain levels of 10^{-6} in exploration seismology. Estimation of the actual interaction volume for an observation system with point sources is also a problem. Nonetheless, the results of these analyses indicate that observable nonlinear effects arising from the interaction of intersecting seismic waves are plausible, and field experiments designed to detect such effects appear feasible.

7. Conclusions

Solutions have been presented for plane wave propagation and interaction of collimated beams in a media characterized by nonlinear elastic constants of the third order. Plane waves propagating through a nonlinear material generate secondary harmonics which increase in amplitude with distance. For P-waves a maximum value is reached while in sensitively related to the amount of attenuation in the medium. For S-waves secondary harmonics are spatially modulated and attain maximum values which are much less sensitive to attenuation. Example calculations for seismology case indicate that large strain rates are necessary before nonlinearity will be detected in most rocks.

If collimated beams intersect in a spherical volume, there are 54 possible combinations of which only 10 result in resonant scattering. Except for the interactions of SH waves, the amplitudes of the scattered waves are directly proportional to the nonlinear elastic constants. The scattered waves form conical beams at specific scattering angles. The width of the beams is directly proportional to the size of the interaction volume and inversely proportional to the scattered wavelength. Though attenuation has not been included in the analyses, example calculations suggest that scattered waves with amplitudes which are a significant proportion of the primary wave amplitude, may arise at moderate strain levels in rock. In addition to the effects of attenuation, further work is required to evaluate the

interaction volume for the more realistic case of point sources in nonlinear media. In this case, the effects of coincident generation of both P- and S- waves by the source must be considered.

Acknowledgments

This work was supported by the Director, Office of Energy Research, Office of Basic Energy Sciences, Engineering and Geosciences Division, of the U.S. Department of Energy under Contract No. DE-AC03-76SF00098.

Appendix I

Nonlinear constants were derived from laboratory velocity measurements on Berea sandstone (Nihei 1991). Hughes and Kelly (1953) derived expressions for velocities assuming third order elastic constants under uniaxial ($\sigma \neq 0$, $\sigma_2 = \sigma_3 = 0$) and hydrostatic ($\sigma = \sigma_2 = \sigma_3 \neq 0$ stress conditions:

$$\rho v_{po}^2 = \lambda + 2\,\mu - \frac{P}{3K}\,[6l + 4m + 7\lambda + 10\mu]$$

$$\rho v_{so}^2 = \mu - 2\,\frac{P}{3K}\,[3m - \frac{1}{2}\,n + 3\,\lambda + 6\mu]$$

$$\rho v_{pz}^2 = \lambda + 2\mu - \frac{T}{3K}[2l + \lambda + \frac{\lambda+\mu}{\mu}(4m + 4\lambda + 10\mu)]$$

$$\rho v_{sz}^2 = \mu - \frac{T}{3K}\,[m + \frac{\lambda n}{4\mu} + 4\lambda + 4\mu]$$

where subscript o refers to hydrostatic and z refers to uniaxial conditions, and P and T are the magnitude of hydrostatic and uniaxial stresses, respectively, and $K = \lambda + \frac{2}{3}\,\mu$. As a consequence of assuming second order nonlinear constants, these equations predict a linear dependence of v^2 on P or T.

Figures A.1 and A.2 present the laboratory data for Berea sandstone. It is seen that the plots are quite nonlinear, meaning that higher order nonlinear constants would be required to describe this behavior. However, since small strains are assumed, it is appropriate to tangent values of the curves at values of mean stresses appropriate to the problem being addressed. For this study both the linear and nonlinear constants were evaluated for low mean stress conditions. Specifically, values of these

constants were derived from the slopes and intercept of the tangent lines shown in the Figures, yielding the values given in section 5.

References

Beresnev I.A., 1993, Interaction of two spherical elastic waves in a nonlinear five-constant medium. J. Acoust.Soc. Am. **94(6)** 3400-3404.

Breazeale M.A. and Thompson D.O., 1963, Finite-amplitude ultrasonic waves in aluminum. Appl. Phys. Lett., **3,** 77-78.

Carr P.H., 1964, Harmonic generation of microwave phonons in quartz. Phys.Rev. Let., **13,** 332-333.

Carr P.H., 1966, Harmonic generation of microwave phonons by radiation pressure and by the phonon phonon interaction. IEEE Trans. Sonics-Ultrasonics, **SU-13,** 103

Daley T.M., Peterson J.E. and McEvilly T.M., 1992, A search for evidence of nonlinear elasticity in the earth. - Science report, DOE, LBL-33313, UC-403 60p.

Ermilin K.K., Zarembo L.K. and Krasil'nikov V.A., 1970, Generation of super high frequency acoustic harmonics in a lithium niobate crystal. Soviet Physics- Solid State, **12,** 1045-1052.

Gedroits A.A. and Krasil'nikov V.A., 1963, Finite-amplitude elastic waves amplitude in solids and deviations from the Hook's law. Zh.Eksp. Teor.Fiz. (Sov. Phys.-JETP), **16,** 1122

Gol'dberg Z.A., 1961, Interaction of plane longitudinal and transverse elastic waves. - Soviet Phys.-Acoust., **Vol.6,#3,** 306-310.

Johnson P.A., McCall K.R. , 1994 , Observation and implications of nonlinear elastic wave response in rock. Geoph.Res.Let., Vol.21, **3** 165-168.

Johnson P.A. et al. ,1987, Nonlinear generation of elastic waves in crystalline rock. J.G.R., Vol.92, **B5** 3597-3602.

Johnson P.A. and Shankland T.J.,1989, Nonlinear generation of elastic waves in granite and sandstone: continuous wave and travel time observations. J.G.R., Vol.94, **B12,** 17,729-17,733.

Hughes D.S. and Kelly J.L., 1953 , Second-order elastic deformations in solids. - Phys.Rev. **Vol.92,#5,** 1145-1149.

Jones G.L. and Kobett D.R., 1963, Interaction of elastic waves in an isotropic solid. - J.Acoust.Soc.of Am., **Vol.35,#1,** 5-10.

Meegan G. D. et al., 1993, Observations of nonlinear elastic wave behavior in sandstone, J. Acoust.Soc. Am. **94(6)** 3387-3391.

Landau L.D. and Lifshitz E.M., 1953, Theory of elasticity New York, John Wiley.

McCall K.R. , 1993, Theoretical study of nonlinear wave propagation. J. Geoph. Res., Vol.99, **B2** 2591-2600.

Moriamez M. et al., 1968, Sur la production harmonique d'hypersons. Comptes rendus Acad.Sc., **267, #22,** B1195-1198.

Murnaghan F.D.,1951. Finite deformation of elastic solid. New York, John Wiley.

Novozhilov V.V., 1953, Foundations of the nonlinear theory of elasticity. Rochester, N.Y. (Translated from Russian edition, 1948) Solid state, 219 p.

Polyakova A.L., 1964, Nonlinear effects in a solid. - Sov.Phys. - Solid state, **Vol.6,#1,** 50-54.

Rollins F.R. , Taylor L.H. and Todd P.H. , 1964, Ultrasonic study of three-phonon interactions. II. Experimental results , Phys. Rew., Vol.136, **3A** A597-A601.

Taylor L.H. and Rollins F.R., 1964, Ultrasonic study of three-phonon interactions. I. Theory , Phys. Rew., Vol.136, **3A** A591-A596.

Thery P. et al., 1969, Production de la seconde harmonique d'une onde hypersonore dans le niobate de lithium, Comptes rendus Acad.Sc., **268, #4,** B285-288.

Zabolotskaya E. A. , 1986, Sound beams in a nonlinear isotropic solid, Sov. Phys. Acoust. **32** 296-299.

Zarembo L.K. and Krasil'nikov V.A., 1966, Introduction in nonlinear acoustics. - In Russian,Moscow,Science, 520.

Zarembo L.K. and Krasil'nikov V.A., 1971, Nonlinear phenomena in the propagation of elastic waves in solids. - Soviet Physics Uspekhi, **Vol.13,#6,** 778-797.

Figure Captions

Figure 1 Resonant conditions and angle definitions for nonlinear interaction of elastic waves for sum frequency generation.

Figure 2 Resonant conditions and angle definitions for nonlinear interaction of elastic waves for difference frequency generation.

Figure 3 Interaction of two plane waves in a volume of nonlinear elastic material.

Figure 4.1 Nonlinear amplitude coefficient and interaction angles for interaction $P(\omega_1) + SV(\omega_2) = P(\omega_1+\omega_2)$.

Figure 4.2 Nonlinear amplitude coefficient and interaction angles for interaction $SV(\omega_1) + SV(\omega_2) = P(\omega_1+\omega_2)$.

Figure 4.3 Nonlinear amplitude coefficient and interaction angles for interaction $SH(\omega_1) + SH(\omega_2) = P(\omega_1+\omega_2)$.

Figure 4.4 Nonlinear amplitude coefficient and interaction angles for interaction $P(\omega_1) + P(\omega_2) = SV(\omega_1-\omega_2)$.

Figure 4.5 Nonlinear amplitude coefficient and interaction angles for interaction $P(\omega_1) + SV(\omega_2) = P(\omega_1-\omega_2)$.

Figure 4.6 Nonlinear amplitude coefficient and interaction angles for interaction $P(\omega_1) + SV(\omega_2) = SV(\omega_1-\omega_2)$.

Figure 4.7 Nonlinear amplitude coefficient and interaction angles for interaction $P(\omega_1) + SH(\omega_2) = SH(\omega_1-\omega_2)$.

Figure 5.1 Normalized scattering amplitude for spherical interaction volume, when $R/\lambda_r = 0.5$.

Figure 5.2 Normalized scattering amplitude for spherical interaction volume, when $R/\lambda_r = 2.0$.

Figure 6.1 Nonlinear amplitude coefficient vs propagation distance for single P- wave propagation for attenuation coefficient $a_p = 10^{-4}(a), 5\cdot 10^{-5}(b), 10^{5}(c), 5\cdot 10^{-6}(d), 10^{6}(e)[cm^{-1}]$.

Figure 6.2 Nonlinear amplitude coefficient vs propagation distance for single S- wave propagation for attenuation coefficient $a_s = 10^{-4}(a), 5\cdot 10^{-5}(b), 10^{5}(c), 5\cdot 10^{-6}(d), 10^{6}(e)[cm^{-1}]$.

Figure A.1 Velocity of P-wave in prestressed sandstone.

Figure A.2 Velocity of S-wave in prestressed sandstone.

Table 1

Forbidden and allowed scattering processes for an isotropic solid

No.	Interaction waves		Scattered waves					
			$\omega_1 + \omega_2$			$\omega - \omega_2$		
			P	SV	SH	P	SV	SH
1	$P(\omega_1)$	$P(\omega_2)$	→			→	×	O
2	$P(\omega_1)$	$SV(\omega_2)$	×			×	×	O
3	$SV(\omega_1)$	$P(\omega_2)$	×					
4	$SV(\omega_1)$	$SV(\omega_2)$	×	O	O		O	O
5	$SH(\omega_1)$	$SH(\omega_2)$	×	O	O		O	O
6	$P(\omega_1)$	$SH(\omega_2)$	O			O	O	×
7	$SH(\omega_1)$	$P(\omega_2)$	O					
8	$SH(\omega_1)$	$SV(\omega_2)$	O	O	O		O	O
9	$SV(\omega_1)$	$SH(\omega_2)$	O	O	O		O	O

→ - possible only when waves propagate in one direction

× - scattering possible

O - polarisation restriction

blank space - interaction restriction

Table 2

Nonlinear scattering coefficients W of two plane elastic wave interaction

#	Interaction	$\cos\alpha$	d_{min}	d_{max}	Scattering coefficient W
1	$P(\omega_1) + P(\omega_2) \rightarrow P(\omega_1+\omega_2)$	1	0	∞	$-D\frac{1+d}{2}\left[4C_1+2C_2+2C_3+C_4+C_5\right] \approx D(1+d)(2m+l)$
2	$P(\omega_1) + P(\omega_2) \rightarrow P(\omega_1-\omega_2)$	1	0	1	$-D\frac{1-d}{2}\left[4C_1+2C_2+2C_3+C_4+C_5\right] \approx D(1-d)(2m+l)$
3	$P(\omega_1) + P(\omega_2) \rightarrow SV(\omega_1-\omega_2)$	$\frac{1}{\gamma^2}-\frac{1}{2}\left[\frac{1}{d}+d\right]\left[\frac{1}{\gamma^2}-1\right]$	$\frac{1-\gamma}{1+\gamma}$	1	$-D\frac{1+d}{2\gamma}\sin 2\alpha\left[2C_1+C_2+C_3\right] \approx D\frac{(1+d)}{2\gamma}\sin 2\alpha\cdot m$
4	$P(\omega_1) + SV(\omega_2) \rightarrow P(\omega_1+\omega_2)$	$\gamma-\frac{d}{2}\left[\frac{1}{\gamma}-\gamma\right]$	0	$\frac{2\gamma}{1-\gamma}$	$-\frac{D}{\gamma^3}\frac{\sin\alpha}{1+d}\left[C_1(3d\gamma+2q)+C_2q+C_3(d\gamma+q)+d\gamma C_5\right] \approx \frac{D}{\gamma^3}\frac{\sin\alpha}{1+d}(\gamma d+q)\cdot m$ $q = \cos\alpha\,(2\gamma d\cos\alpha + d^2 + 2\gamma^2)$
5	$P(\omega_1) + SV(\omega_2) \rightarrow P(\omega_1-\omega_2)$	$\gamma+\frac{d}{2}\left[\frac{1}{\gamma}-\gamma\right]$	0	$\frac{2\gamma}{1+\gamma}$	$-\frac{D}{\gamma^3}\frac{\sin\alpha}{1-d}\left[C_1(3d\gamma+2q)+C_2q+C_3(d\gamma+q)+d\gamma C_5\right] \approx \frac{D}{\gamma^3}\frac{\sin\alpha}{1-d}(\gamma d+q)\cdot m$ $q = \cos\alpha\,(2\gamma d\cos\alpha - d^2 - 2\gamma^2)$

Table 2 (continued)

#	Interaction	$\cos\alpha$	d_{min}	d_{max}	Scattering coefficient W
6	$P(\omega_1) + SV(\omega_2)$ $\rightarrow SV(\omega_1-\omega_2)$	$\frac{1}{\gamma}-\frac{1}{2d}\left[\frac{1}{\gamma}-\gamma\right]$	$\frac{1-\gamma}{2}$	$\frac{1+\gamma}{2}$	$\frac{D}{\gamma^5}\left[C_1(q(d-q)+\gamma^2\sin^2\alpha) - C_2 q\gamma\cos\alpha + C_3\gamma^2\sin^2\alpha + C_5 dq)\right]$ $\approx -\frac{D}{\gamma^5}(2d\gamma\cos\alpha - d^2-\gamma^2\cos 2\alpha)\cdot\frac{m}{2}$ $q = \gamma\cos\alpha - d$
7	$SV(\omega_1) + P(\omega_2)$ $\rightarrow P(\omega_1+\omega_2)$	$\gamma - \frac{1}{2d}\left[\frac{1}{\gamma}-\gamma\right]$	$\frac{1-\gamma}{2\gamma}$	∞	$\frac{D}{\gamma^3}\frac{\sin\alpha}{1+d}\left[C_1(3d\gamma+2q)+C_2 q+C_3(d\gamma+q)+d\gamma C_5\right]$ $\approx -D\frac{\sin\alpha}{\gamma}\frac{1+2d}{1+d}(\gamma d + \cos\alpha)\cdot m$ $q = \cos\alpha\,(2\gamma d\cos\alpha + 1 + 2\gamma^2 d^2)$
8	$SV(\omega_1) + SV(\omega_2)$ $\rightarrow P(\omega_1+\omega_2)$	$\gamma^2+\frac{1}{2}\left[\frac{1}{d}+d\right]\left[\gamma^2-1\right]$	$\frac{1-\gamma}{1+\gamma}$	$\frac{1+\gamma}{1-\gamma}$	$D\frac{(1+d)}{\gamma^2}\left[(C_1\cos 2\alpha+C_2\cos^2\alpha-C_3\sin^2\alpha\right]$ $\approx -D\frac{(1+d)}{2\gamma^2}\cos 2\alpha\cdot m$
9	$SH(\omega_1) + SH(\omega_2)$ $\rightarrow P(\omega_1+\omega_2)$	$\gamma^2+\frac{1}{2}\left[\frac{1}{d}+d\right]\left[\gamma^2-1\right]$	$\frac{1-\gamma}{1+\gamma}$	$\frac{1+\gamma}{1-\gamma}$	$D\frac{(1+d)}{\gamma^2}\left[(C_1+C_2)\cos\alpha+C_1\frac{2d\sin^2\alpha}{\gamma^2(1+d)^2}\right]$ $\approx -D\frac{(1+d)}{2\gamma^2}\left[m\cos\alpha + n\frac{d\sin^2\alpha}{2\gamma^2(1+d)^2}\right]$
10	$P(\omega_1) + SH(\omega_2)$ $\rightarrow SH(\omega_1-\omega_2)$	$\frac{1}{\gamma}-\frac{1}{2d}\left[\frac{1}{\gamma}-\gamma\right]$	$\frac{1-\gamma}{2}$	$\frac{1+\gamma}{2}$	$\frac{D}{\gamma^3}\left[C_1\cos\alpha(2\frac{d}{\gamma}\cos\alpha-1)-C_2\cos\alpha+C_5\frac{d}{\gamma}\right]$ $\approx -\frac{D}{2\gamma^3}\left[m\,(\frac{d}{\gamma}-\cos\alpha) - n\,\frac{d}{2\gamma}\sin^2\alpha\right]$

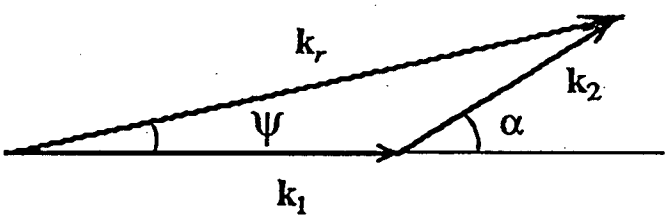

$$\omega_r = \omega_1 + \omega_2$$

$$\mathbf{k}_r = \mathbf{k}_1 + \mathbf{k}_2$$

Fig. 1

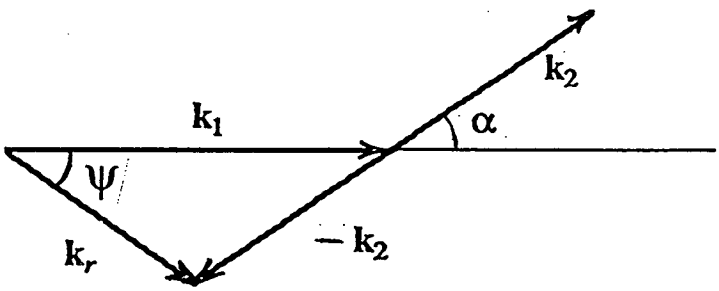

$$\omega_r = \omega_1 - \omega_2$$

$$\mathbf{k}_r = \mathbf{k}_1 - \mathbf{k}_2$$

Fig.2

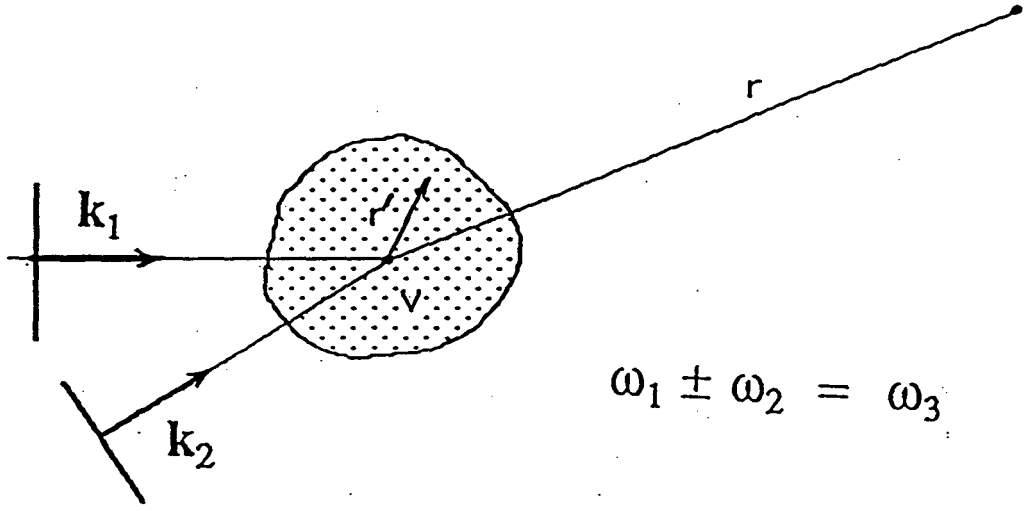

$$\omega_1 \pm \omega_2 = \omega_3$$

Fig. 3

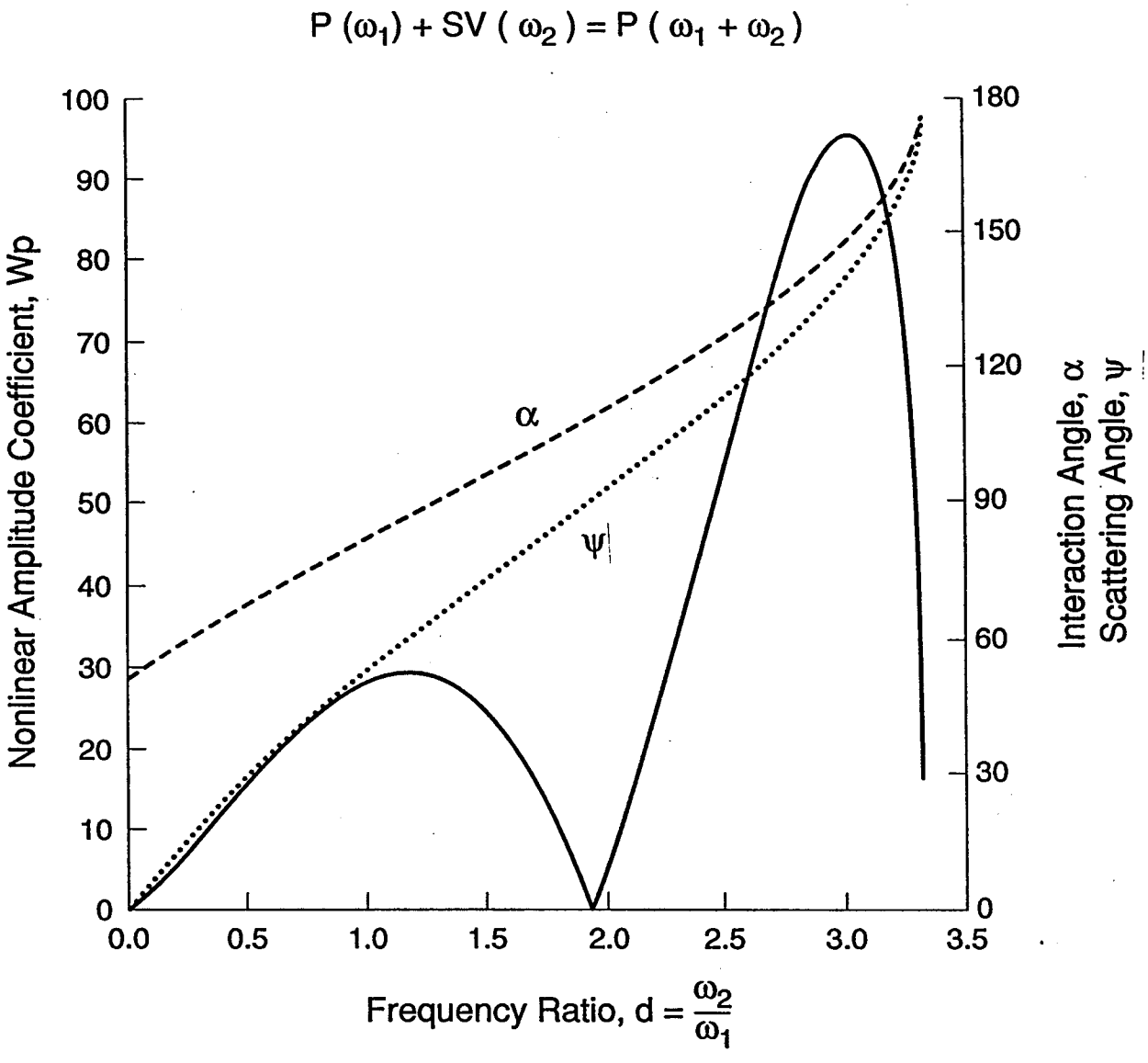
P (ω1) + SV (ω2) = P (ω1 + ω2)
Nonlinear Amplitude Coefficient, Wp
Interaction Angle, α
Scattering Angle, ψ
α
ψ
100
90
80
70
60
50
40
30
20
10
0
180
150
120
90
60
30
0
0.0
0.5
1.0
1.5
2.0
2.5
3.0
3.5
Frequency Ratio, d = ω2/ω1

Fig. 4.1

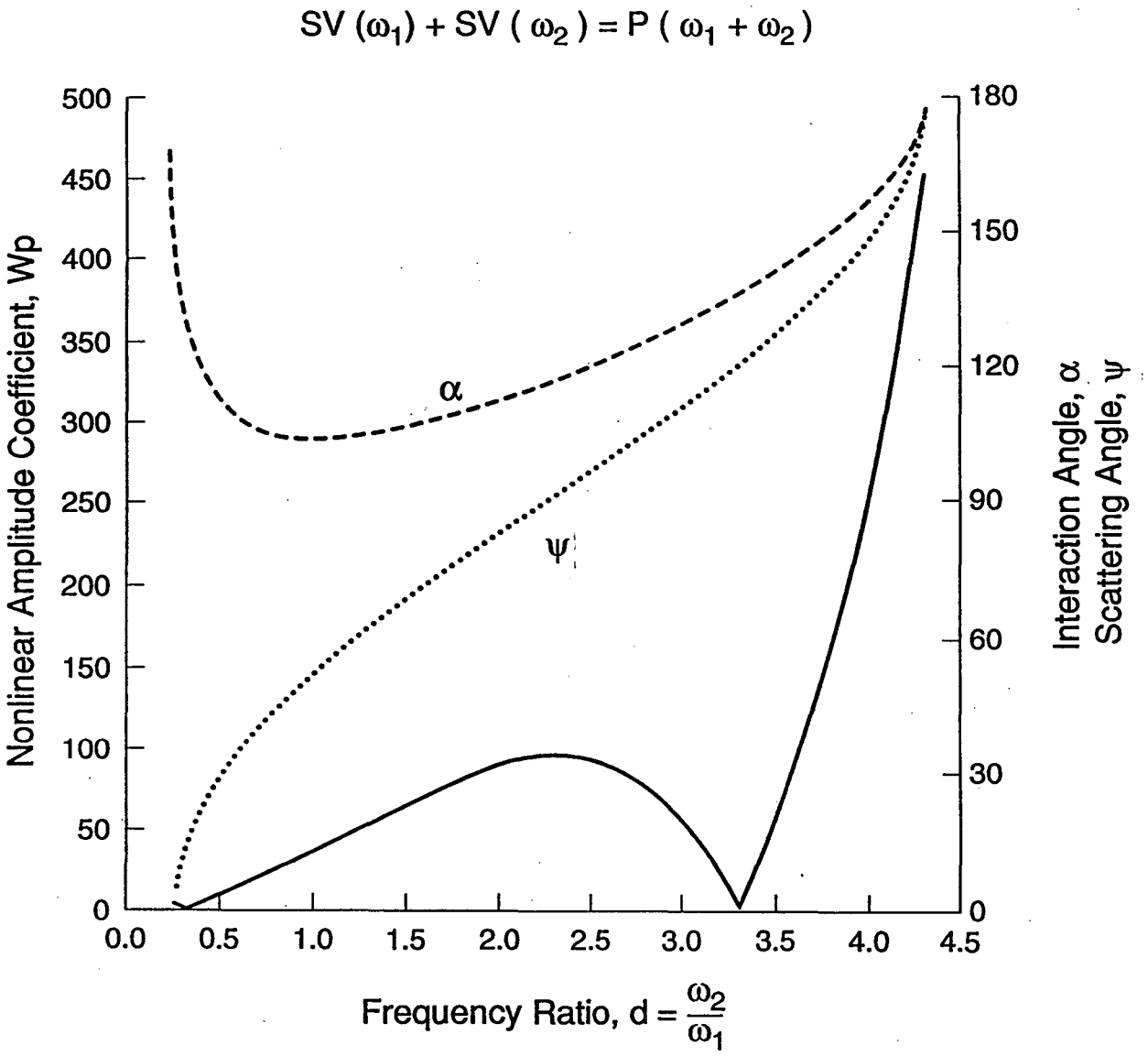
SV (ω1) + SV (ω2) = P (ω1 + ω2)
Nonlinear Amplitude Coefficient, Wp
Interaction Angle, α
Scattering Angle, ψ
α
ψ
Frequency Ratio, d = ω2/ω1
0
50
100
150
200
250
300
350
400
450
500
0
30
60
90
120
150
180
0.0
0.5
1.0
1.5
2.0
2.5
3.0
3.5
4.0
4.5

Fig. 4.2

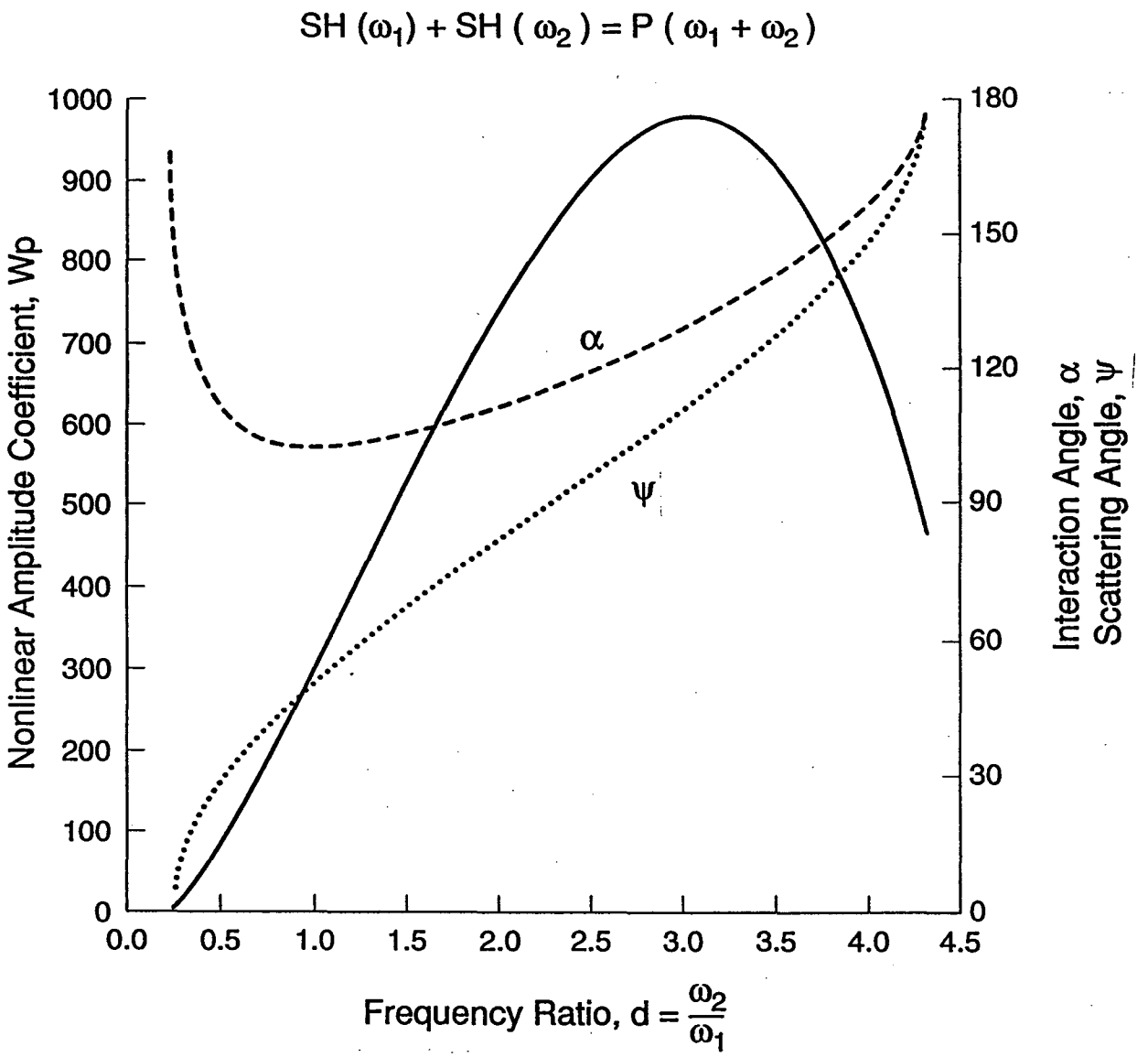
SH (ω1) + SH (ω2) = P (ω1 + ω2)
Nonlinear Amplitude Coefficient, Wp
Interaction Angle, α
Scattering Angle, ψ
α
ψ
1000
900
800
700
600
500
400
300
200
100
0
180
150
120
90
60
30
0
0.0
0.5
1.0
1.5
2.0
2.5
3.0
3.5
4.0
4.5
Frequency Ratio, d = ω2/ω1

Fig. 4.3

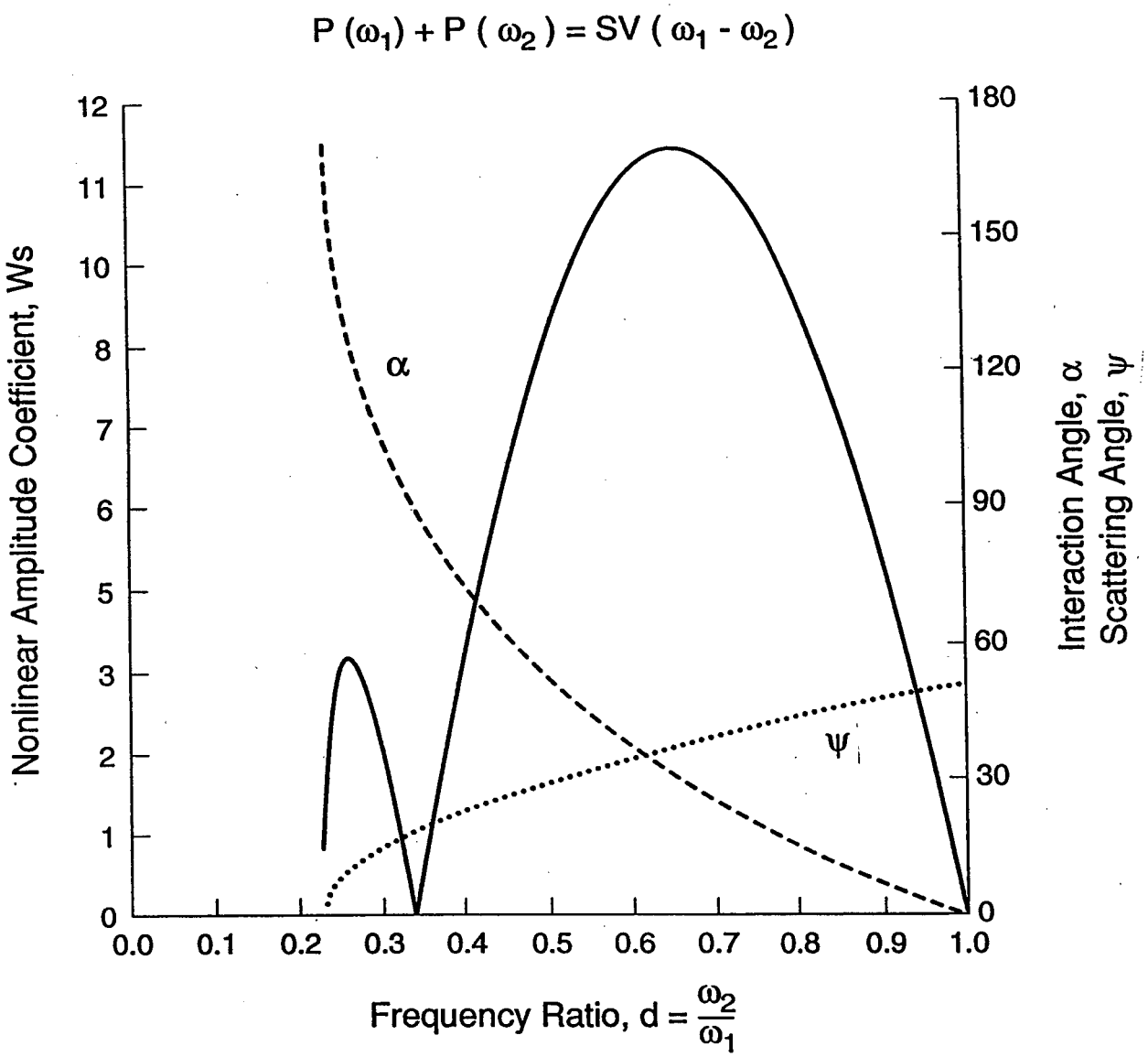
P (ω1) + P (ω2) = SV (ω1 - ω2)
Nonlinear Amplitude Coefficient, Ws
Interaction Angle, α
Scattering Angle, ψ
α
ψ
Frequency Ratio, d = ω2/ω1
0
1
2
3
5
6
7
8
10
11
12
0
30
60
90
120
150
180
0.0
0.1
0.2
0.3
0.4
0.5
0.6
0.7
0.8
0.9
1.0

Fig. 4.4

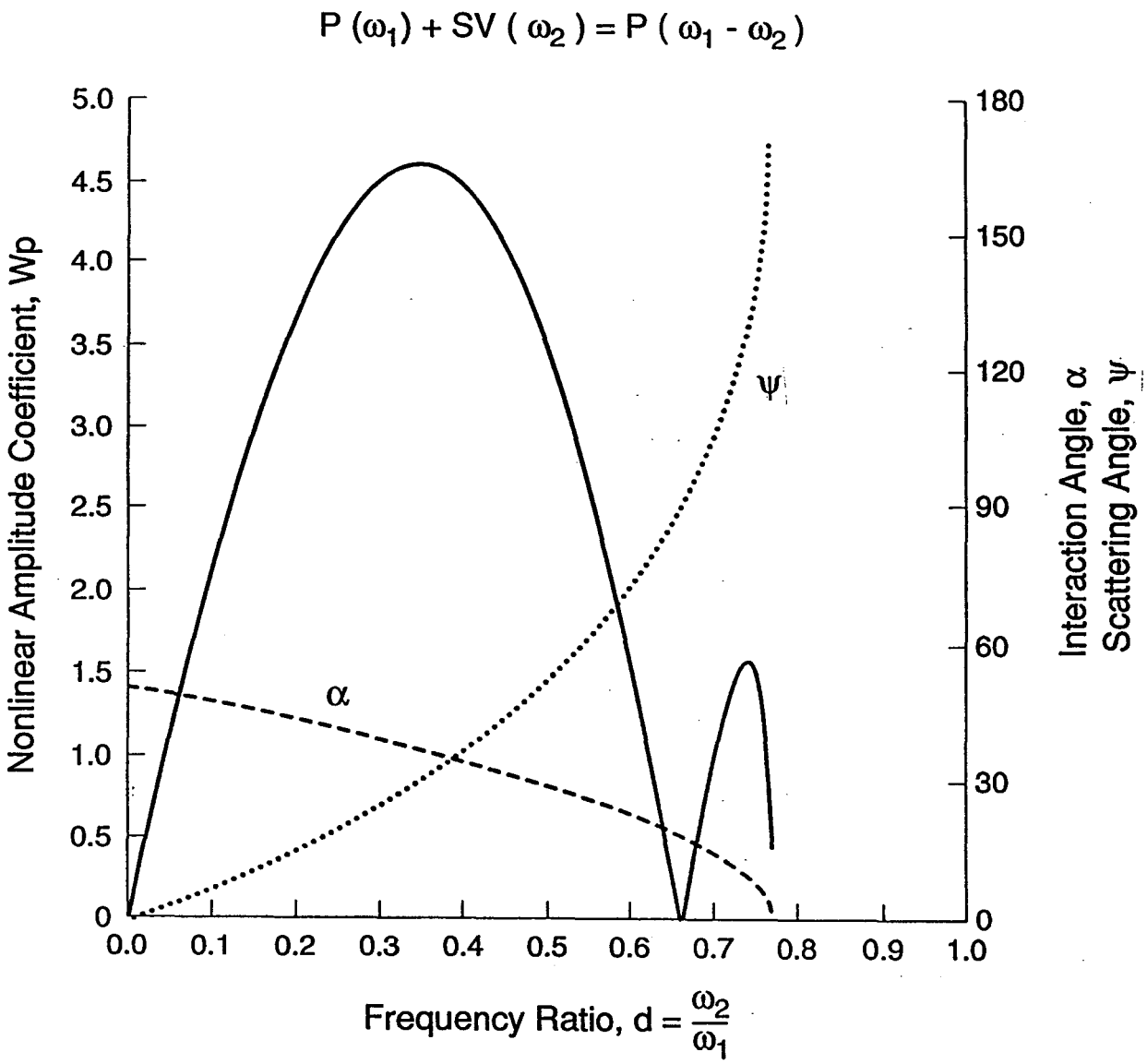
P (ω1) + SV (ω2) = P (ω1 - ω2)
Nonlinear Amplitude Coefficient, Wp
Interaction Angle, α
Scattering Angle, ψ
Frequency Ratio, d = ω2/ω1
α
ψ
5.0
4.5
4.0
3.5
3.0
2.5
2.0
1.5
1.0
0.5
0
180
150
120
90
60
30
0
0.0
0.1
0.2
0.3
0.4
0.5
0.6
0.7
0.8
0.9
1.0

Fig. 4.5

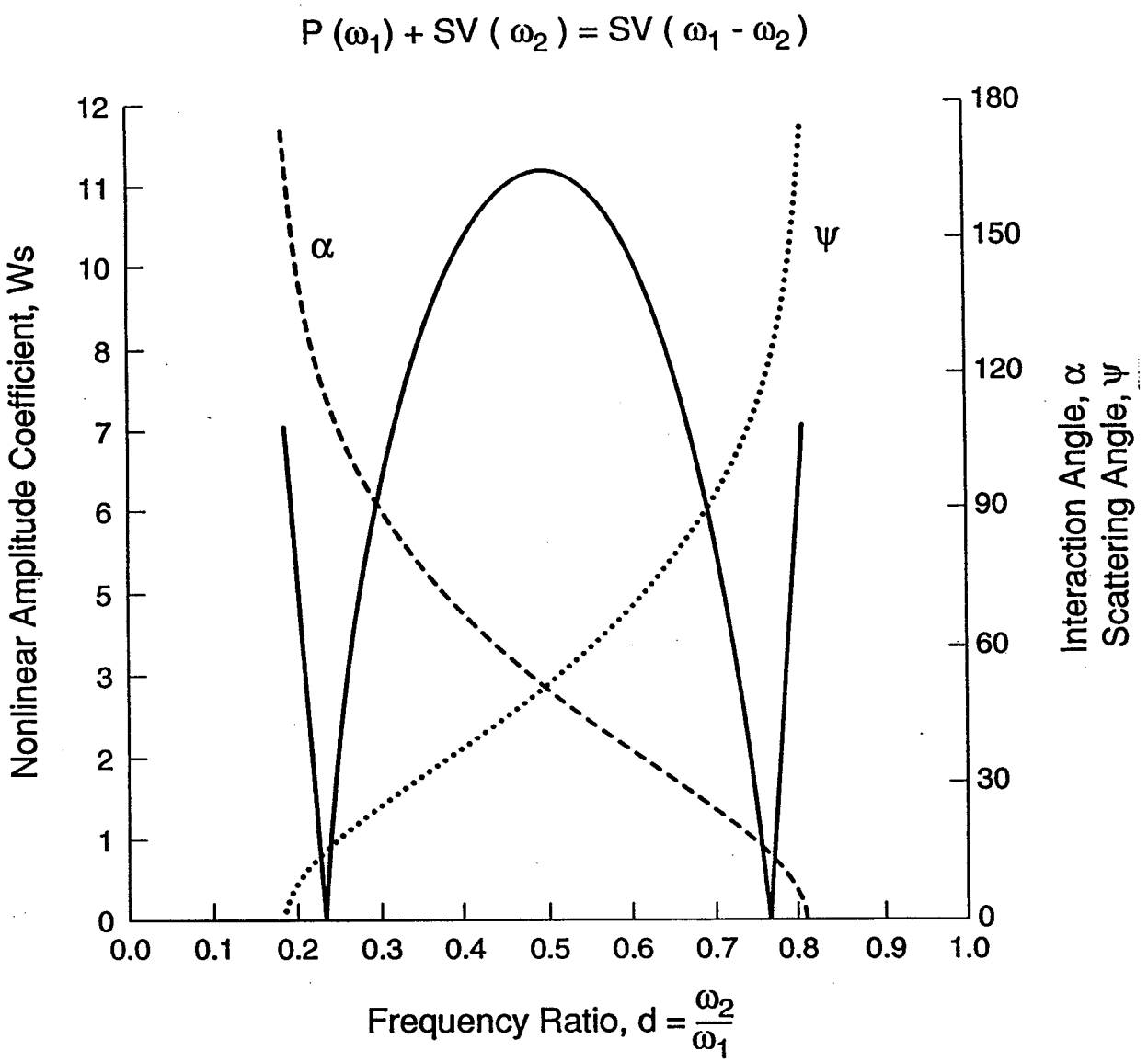
P (ω1) + SV (ω2) = SV (ω1 - ω2)
Nonlinear Amplitude Coefficient, Ws
Interaction Angle, α
Scattering Angle, ψ
α
ψ
Frequency Ratio, d = ω2/ω1
0
1
2
3
5
6
7
8
10
11
12
0
30
60
90
120
150
180
0.0
0.1
0.2
0.3
0.4
0.5
0.6
0.7
0.8
0.9
1.0

Fig. 4.6

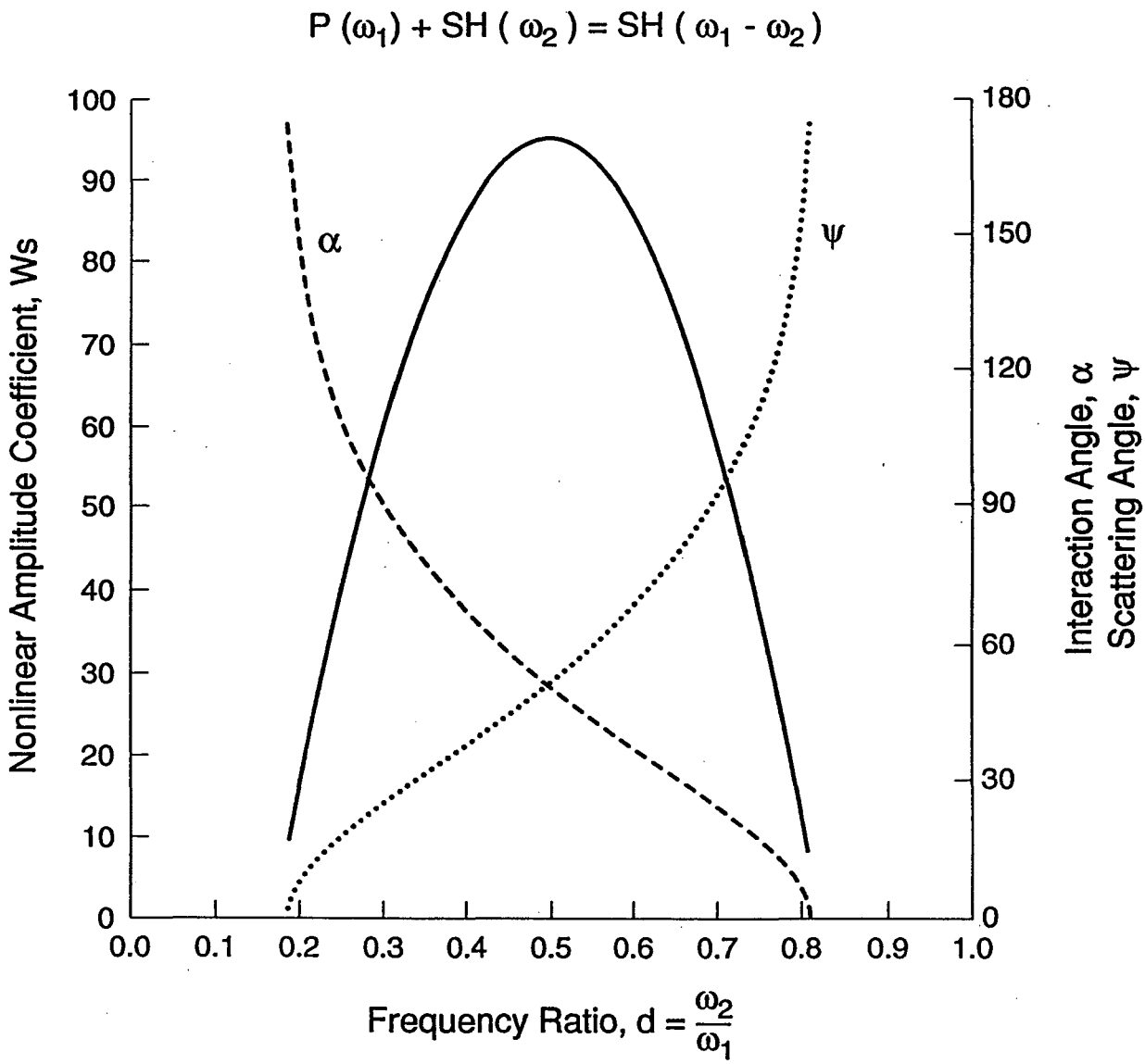
P (ω1) + SH (ω2) = SH (ω1 - ω2)
Nonlinear Amplitude Coefficient, Ws
Interaction Angle, α
Scattering Angle, ψ
Frequency Ratio, d = ω2/ω1
α
ψ
100
90
80
70
60
50
40
30
20
10
0
180
150
120
90
60
30
0
0.0
0.1
0.2
0.3
0.4
0.5
0.6
0.7
0.8
0.9
1.0

Fig. 4.7

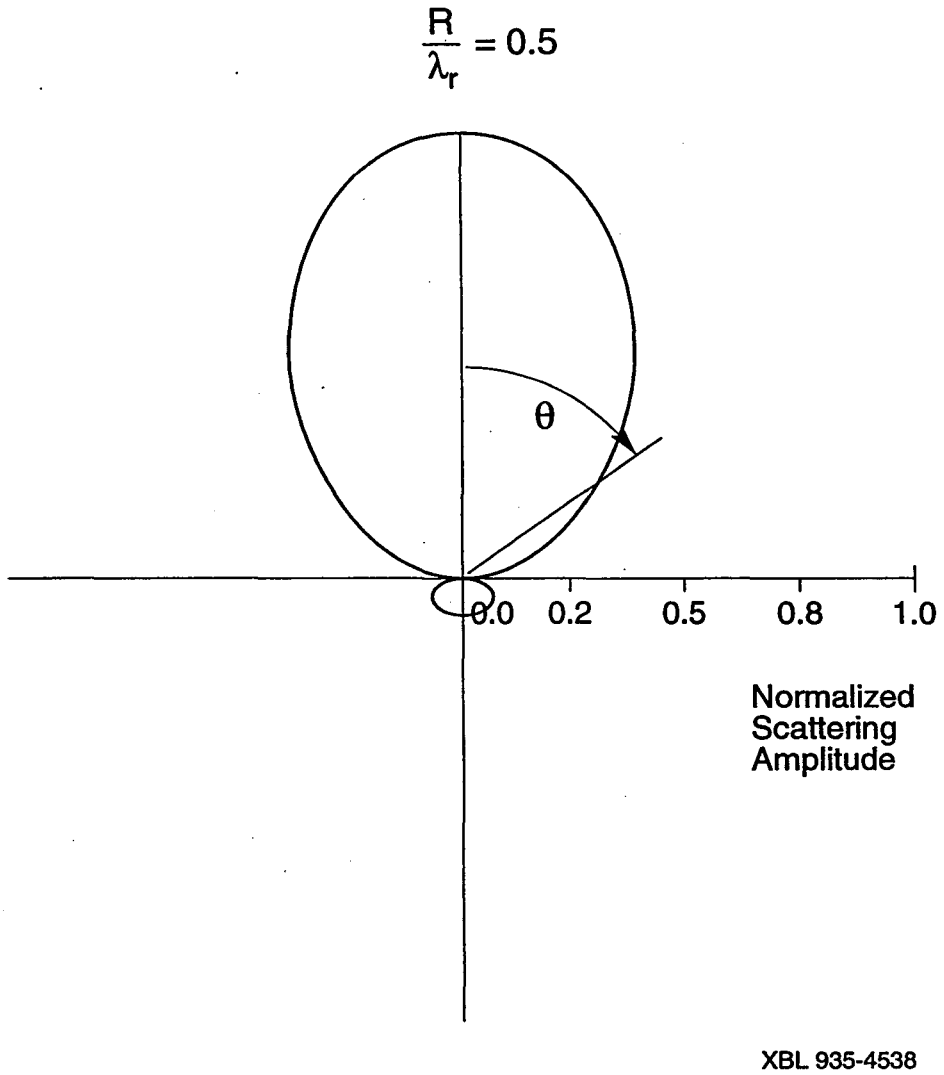
$\frac{R}{\lambda_r} = 0.5$
θ
0.0
0.2
0.5
0.8
1.0
Normalized
Scattering
Amplitude
XBL 935-4538

Fig. 5.1

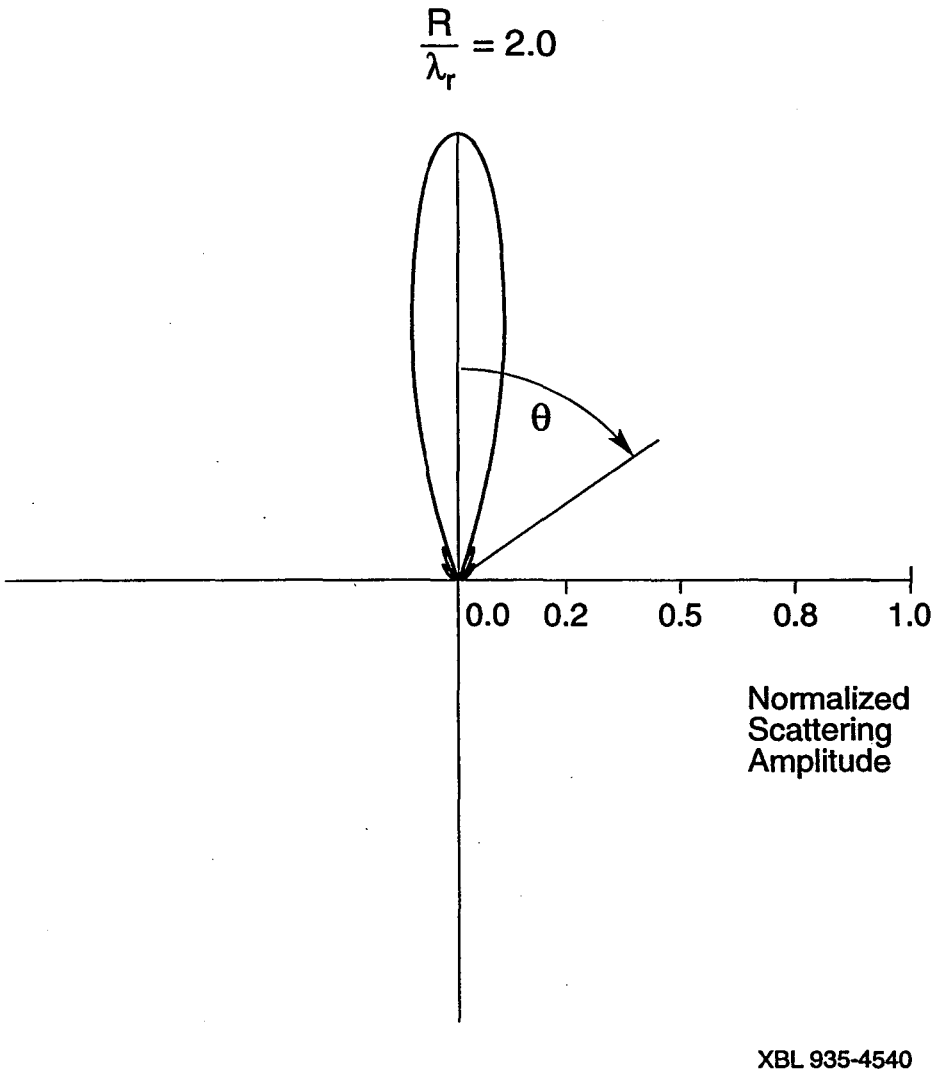
$\frac{R}{\lambda_r} = 2.0$
θ
0.0
0.2
0.5
0.8
1.0
Normalized
Scattering
Amplitude
XBL 935-4540

Fig. 5.2

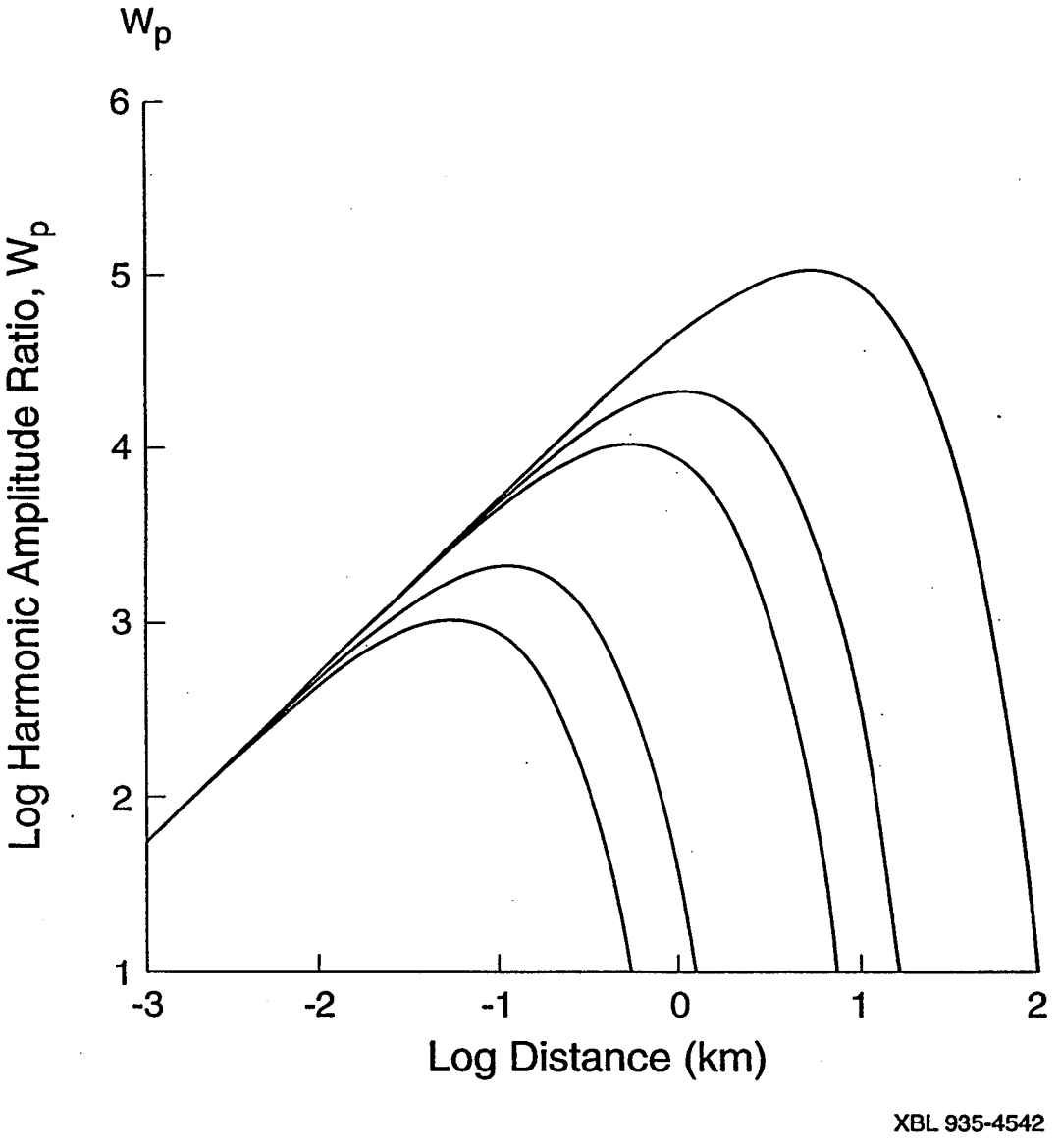
W_p
6
5
4
3
2
1
Log Harmonic Amplitude Ratio, W_p
-3
-2
-1
0
1
2
Log Distance (km)
XBL 935-4542

Fig. 6.1

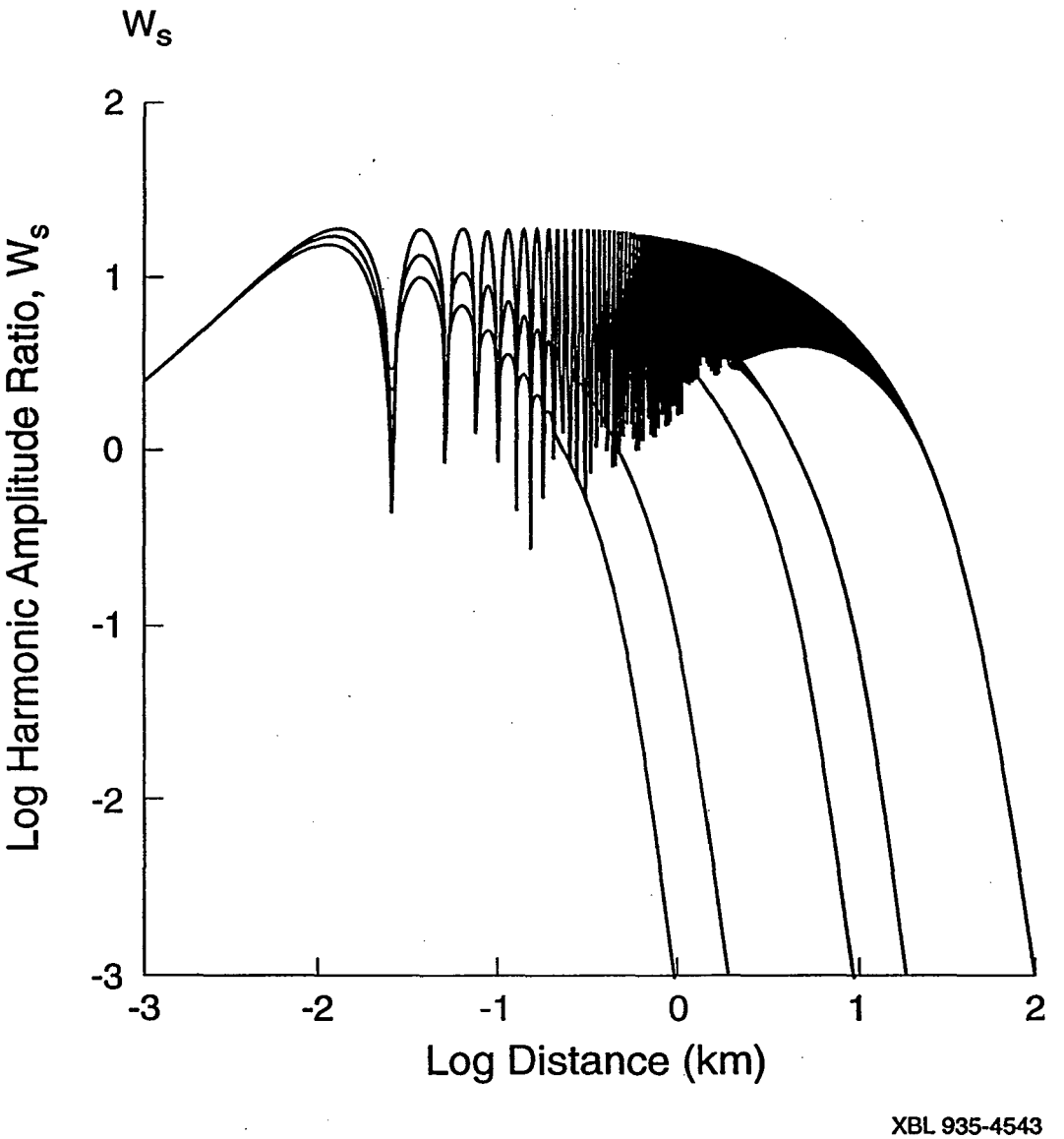
W_s
2
1
0
-1
-2
-3
Log Harmonic Amplitude Ratio, W_s
-3
-2
-1
0
1
2
Log Distance (km)
XBL 935-4543

Fig. 6.2

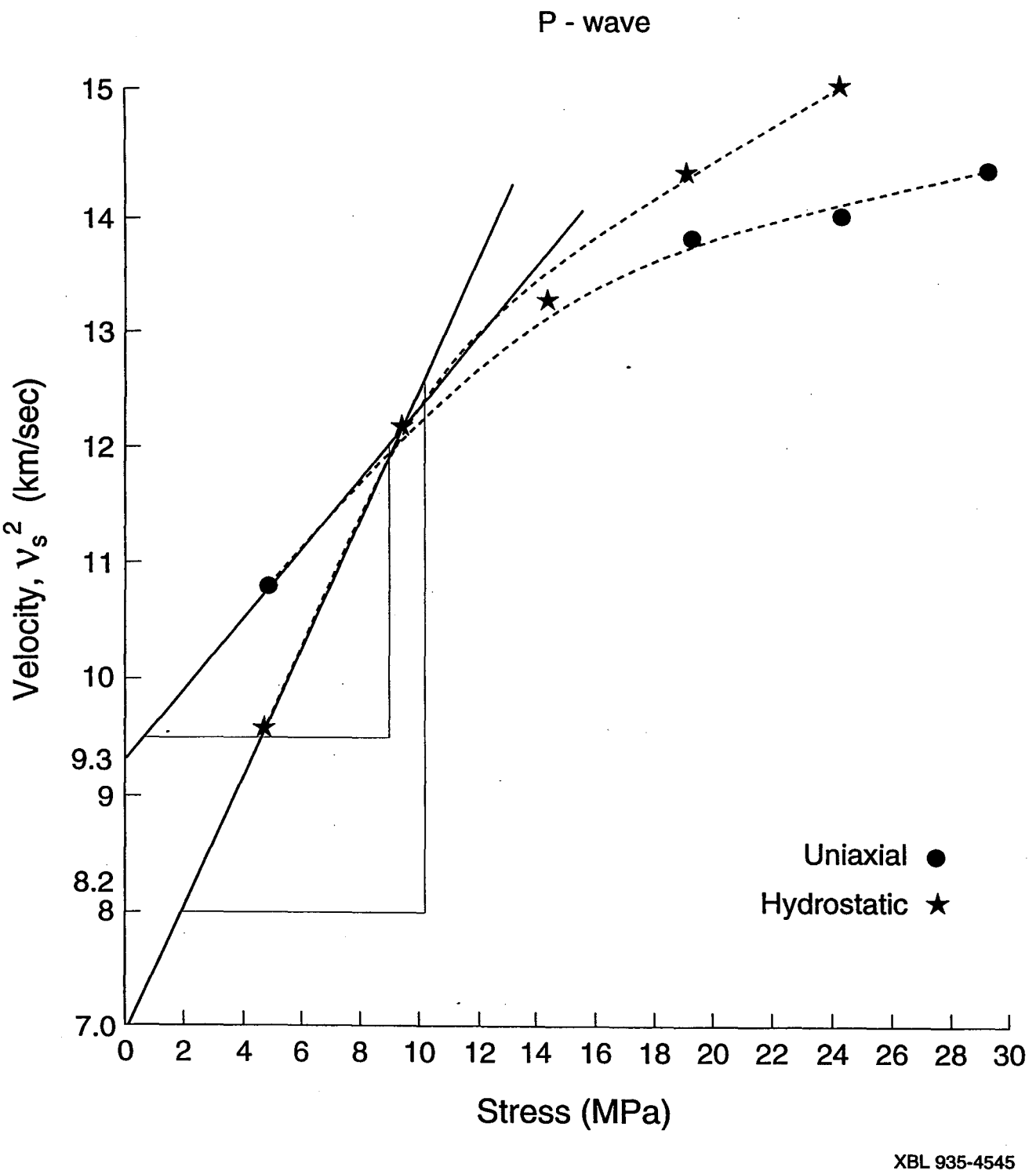
P - wave
Velocity, V_s^2 (km/sec)
15
14
13
12
11
10
9.3
9
8.2
8
7.0
0
2
4
6
8
10
12
14
16
18
20
22
24
26
28
30
Stress (MPa)
Uniaxial
Hydrostatic
XBL 935-4545

Fig. A.1

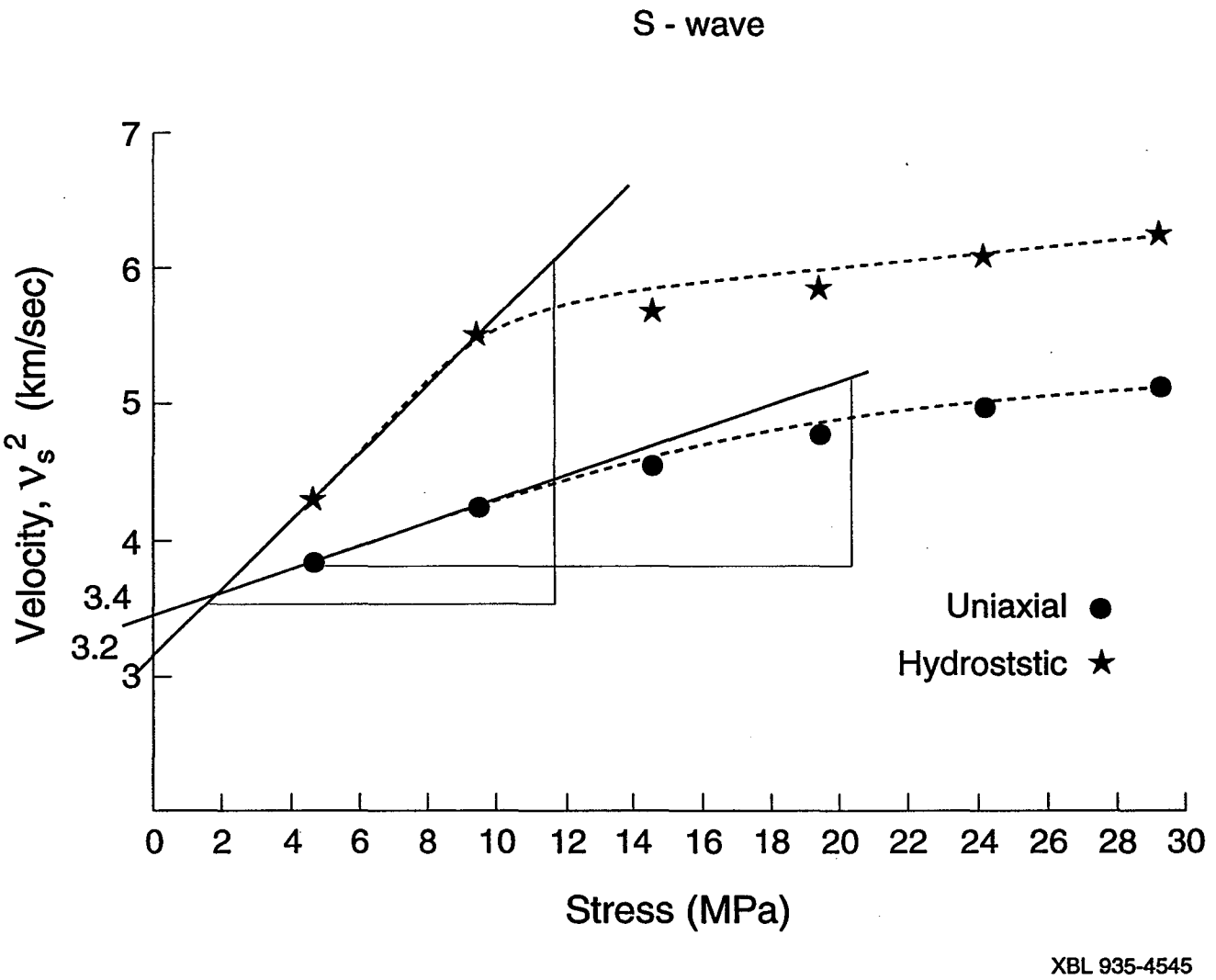
S - wave
Velocity, v_s^2 (km/sec)
7
6
5
4
3.4
3.2
3
0
2
4
6
8
10
12
14
16
18
20
22
24
26
28
30
Stress (MPa)
Uniaxial
Hydroststic
XBL 935-4545

Fig. A.2

Ernest Orlando Lawrence Berkeley National Laboratory
One Cyclotron Road | Berkeley, California 94720

Prepared for the U.S. Department of Energy under Contract No. DE-AC03-76SF00098